MOLECULAR AND CELLULAR BIOLOGY, Nov. 2005, p. 9554–9575 Vol. 25, No. 21
0270-7306/05/$08.00+0 doi:10.1128/MCB.25.21.9554–9575.2005

AMP-Activated Protein Kinase Protects Cardiomyocytes against Hypoxic Injury through Attenuation of Endoplasmic Reticulum Stress

Kazuo Terai,[1] Yoshimune Hiramoto,[1] Mitsuru Masaki,[1] Shoko Sugiyama,[1] Tadashi Kuroda,[1] Masatsugu Hori,[1] Ichiro Kawase,[2] and Hisao Hirota[1]*

Department of Cardiovascular Medicine[1] and Respiratory Medicine and Rheumatic Diseases,[2] Osaka University Graduate School of Medicine, Suita City, Osaka 565-0871, Japan

Received 6 June 2005/Returned for modification 30 June 2005/Accepted 16 August 2005

Oxygen deprivation leads to the accumulation of misfolded proteins in the endoplasmic reticulum (ER), causing ER stress. Under conditions of ER stress, inhibition of protein synthesis and up-regulation of ER chaperone expression reduce the misfolded proteins in the ER. AMP-activated protein kinase (AMPK) is a key regulatory enzyme involved in energy homeostasis during hypoxia. It has been shown that AMPK activation is associated with inhibition of protein synthesis via phosphorylation of elongation factor 2 (eEF2) in cardiomyocytes. We therefore examined whether AMPK attenuates hypoxia-induced ER stress in neonatal rat cardiomyocytes. We found that hypoxia induced ER stress, as assessed by the expression of CHOP and BiP and cleavage of caspase 12. Knockdown of CHOP or caspase 12 through small interfering RNA (siRNA) resulted in decreased expression of cleaved poly(ADP-ribose) polymerase following exposure to hypoxia. We also found that hypoxia-induced CHOP expression and cleavage of caspase 12 were significantly inhibited by pretreatment with 5-aminoimidazole-4-carboxyamide-1-β-D-ribofuranoside (AICAR), a pharmacological activator of AMPK. In parallel, adenovirus expressing dominant-negative AMPK significantly attenuated the cardioprotective effects of AICAR. Knockdown of eEF2 phosphorylation using eEF2 kinase siRNA abolished these cardioprotective effects of AICAR. Taken together, these findings demonstrate that activation of AMPK contributes to protection of the heart against hypoxic injury through attenuation of ER stress and that attenuation of protein synthesis via eEF2 inactivation may be the mechanism of cardioprotection by AMPK.

The mitochondrion is considered the central organelle in the intrinsic apoptotic pathway. However, accumulating evidence suggests that other organelles, including the endoplasmic reticulum (ER), lysosomes, and Golgi apparatus, are also major points of integration of proapoptotic signaling or damage sensing (10, 14). In particular, in the myocardium, the ER participates in maintenance of cellular calcium homeostasis (57) and synthesis of secretory proteins (16) such as atrial natriuretic peptide, brain natriuretic peptide (15), and vascular endothelial growth factor (VEGF) (51). Dysfunction of the ER might thus contribute to the pathogenesis of heart disease.

Various stimuli collectively known as ER stress, such as ischemia, hypoxia, oxidative stress, and Ca^{2+} depletion in the ER, can potentially induce accumulation of unfolded or misfolded proteins in the ER of neuronal and pancreatic β-cells (30). When these proteins accumulate in the ER, they must be refolded or degraded to maintain ER homeostasis. Eukaryotic cells have three different mechanisms for dealing with accumulation of unfolded proteins in the ER (43), collectively termed the unfolded protein responses (UPR): (i) in the early phase, translational attenuation occurs to decrease the load in the ER; (ii) in the next phase, transcriptional induction of ER-localized molecular chaperones and folding enzymes occurs to augment the folding capacity in the ER; and (iii) in a later phase, ER-associated protein degradation is induced to eliminate misfolded proteins in the ER by the ubiquitin-proteasome system (64). Mammalian cells determine the fate of unfolded or misfolded proteins in the ER by a time-dependent phase transition mechanism (70). When ER stress conditions persist, however, initiation of apoptotic processes is promoted by transcriptional induction of C/EBP homologous protein (CHOP/GADD153) (50), the caspase 12-dependent pathway (46), and activation of the c-Jun NH2-terminal kinase (JNK)-dependent pathway (65).

AMP-activated protein kinase (AMPK) is highly expressed in heart (59) and is activated by cellular stresses that increase the AMP-to-ATP ratio (24), such as hypoxia/anoxia (55), glucose deprivation (67), and pressure overload hypertrophy (63). If ATP is used up faster than it can be resynthesized, the ATP level falls, with an increase in AMP as a consequence of the reaction catalyzed by adenylate kinase. The corresponding increase in the AMP:ATP ratio triggers the activation of AMPK, leading to the phosphorylation of a large number of downstream targets (22). Once activated, AMPK increases energy supply by switching on ATP-generating pathways and decreases energy demand by switching off ATP-consuming pathways (7). The AMPK cascade appears to regulate cellular energy status during metabolic stress and, in this fashion, exhibits cardioprotective effects (23). Indeed, 5-aminoimidazole-4-carboxamide-1-β-D-ribofuranoside (AICAR), a pharmacological activator of AMPK, has been shown to reduce myocardial ischemic injury in humans and animals (21, 36, 44). AMPK is also activated through AMP-independent pathways by hor-

* Corresponding author. Mailing address: Department of Cardiovascular Medicine, Osaka University Graduate School of Medicine, 2-2, Yamadaoka, Suita City, Osaka 565-0871, Japan. Phone: 81-6-6879-3835. Fax: 81-6-6879-3839. E-mail: hirota@imed3.med.osaka-u.ac.jp.

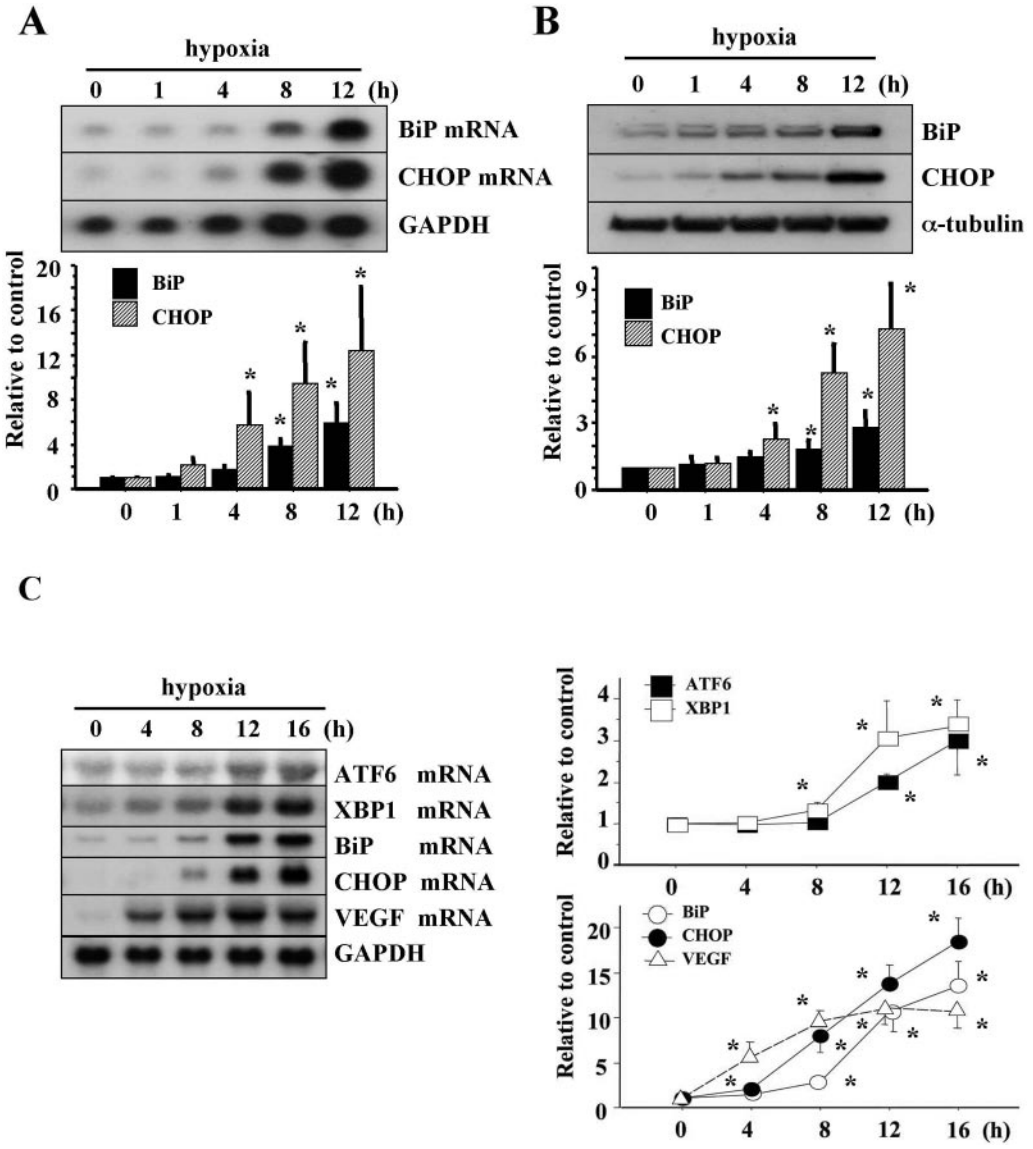

FIG. 1. Unfolded protein responses were induced by hypoxia in cardiomyocytes. Neonatal rat cardiomyocytes were incubated under hypoxic conditions for the indicated time periods as described in Materials and Methods. Expression levels of BiP and CHOP mRNA (A), BiP and CHOP protein (B), and ATF6, XBP1, BiP, CHOP, and VEGF mRNA (C) were examined by Northern blot (A and C) and Western blot (B) analyses. Densitometry was used to determine the ratios of band intensities for BiP and CHOP to band intensities for GAPDH (A and C) and α-tubulin (B). Values are the means ± SDs from three independent experiments. *, P of <0.05 versus without hypoxia.

mones such as leptin (42) and adiponectin (68) and by pharmacological agents such as metformin (72), as well as during osmotic stress (18). Recent reports have shown that these hormones and agents improve cardiovascular function (40, 58). Moreover, mutations of the γ2 regulatory subunit of AMPK have been reported to cause familial hypertrophic cardiomyopathy associated with Wolff-Parkinson-White syndrome and glycogen storage disease (20), suggesting that a genetic defect of activation of AMPK in response to stress might be responsible for susceptibility to development of cardiovascular disease. However, the exact role played by AMPK in mediating cardioprotective effects remains to be determined. Because it has been shown that AMPK activation is associated with inhibition of protein synthesis in cardiomyocytes (28), we speculated that AMPK might have cardioprotective effects against ER stress-mediated cell death.

In the present study, we found that ER stress is one pathological change induced by hypoxia in neonatal rat cardiomyocytes and that it plays a significant role in the process of apoptosis. In addition, we found that AMPK could potentially prevent ER-associated apoptotic signaling in cardiomyocytes. To our knowledge, this is the first demonstration that AMPK is involved in the regulation of the UPR under hypoxic conditions.

MATERIALS AND METHODS

Reagents. AICAR (Toronto Research Chemicals, Inc., Canada) was used as a pharmacological activator of AMPK. Tunicamycin (Tm), an inhibitor of the synthesis of all N-linked glycoproteins, and thapsigargin (Tg), an irreversible

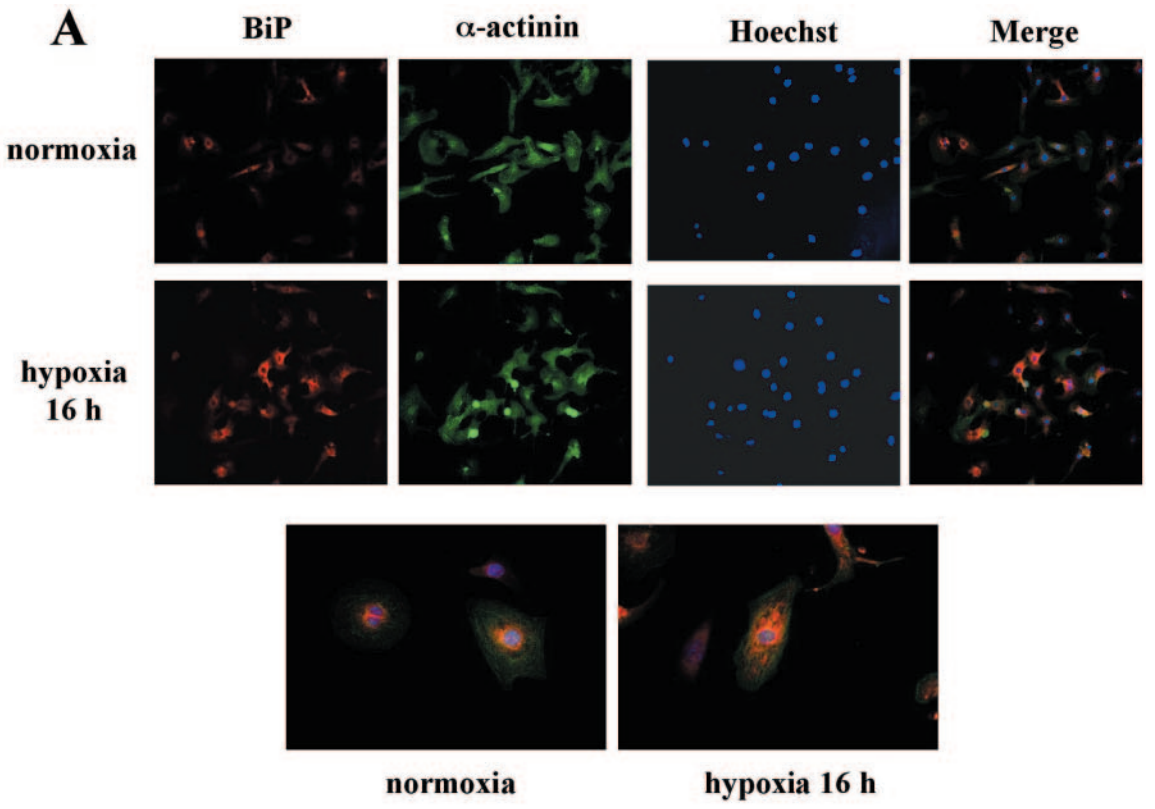
A
BiP
α-actinin
Hoechst
Merge
normoxia
hypoxia 16 h
normoxia
hypoxia 16 h

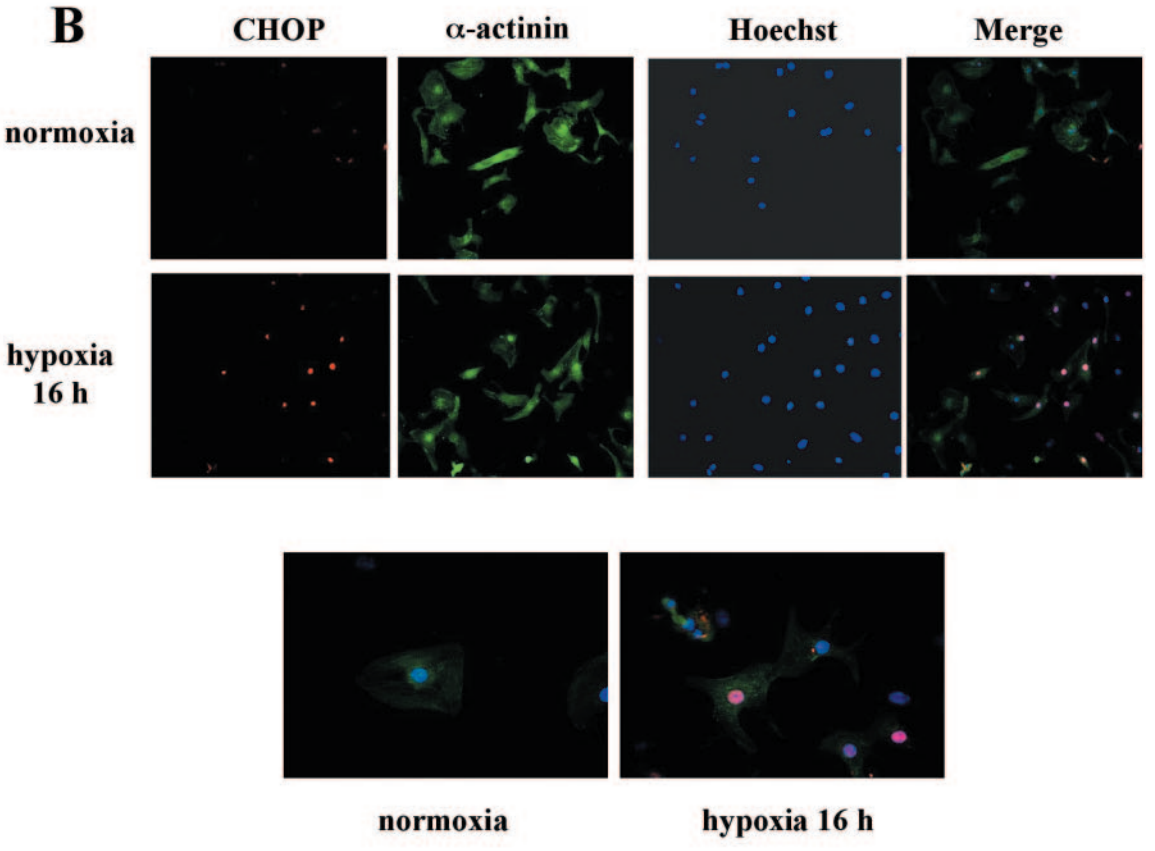
B
CHOP
α-actinin
Hoechst
Merge
normoxia
hypoxia 16 h
normoxia
hypoxia 16 h

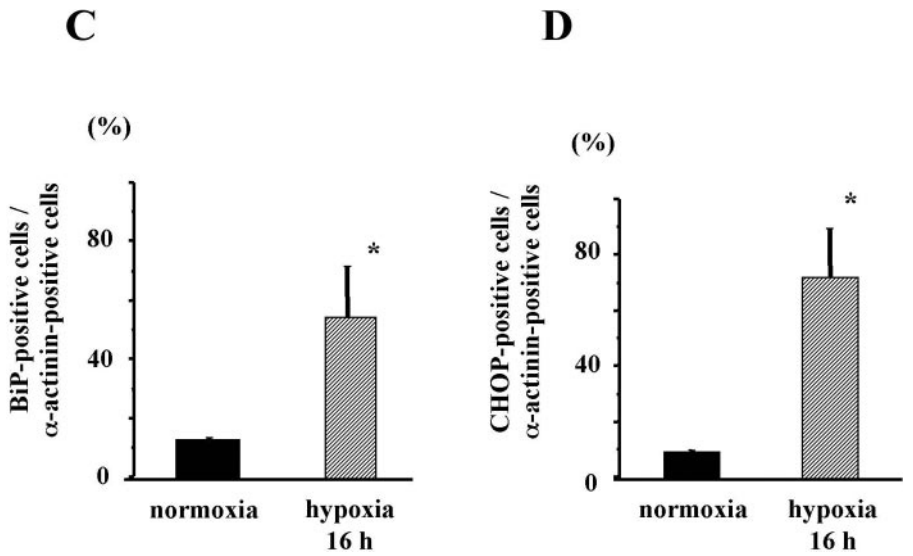

FIG. 2. Immunostaining of BiP and CHOP induced by hypoxia in cardiomyocytes. (A and B) Neonatal rat cardiomyocytes were grown on glass coverslips coated with gelatin and exposed to normoxic or hypoxic conditions for 16 h. Cells were immunostained with anti-BiP (A) or anti-CHOP (B) and anti-sarcomeric α-actinin antibodies and examined microscopically (original magnification of ×200). Hoechst 33258 was used for nuclear staining. Images shown are representative findings from three independent experiments that had similar results. Pictures in bottom row of each panel are of cells triply stained with anti-BiP (A) or anti-CHOP antibody (B), anti-sarcomeric α-actinin antibody, and Hoechst 33258 and viewed at a higher magnification (×400). (C and D) Bars represent the percentages of BiP-positive (C) or CHOP-positive (D) cells among α-actinin-positive cells after exposure to hypoxia for 16 h. MetaMorpho microscope image analysis software was used for quantitative analysis. BiP- and CHOP-positive cells were defined as those of intensities greater than the mean + SD of the control group under normoxic conditions. Values are the means ± SDs from three independent experiments. More than 100 sarcomeric α-actinin-positive cells were examined in each experiment. *, P of <0.05 versus control.

inhibitor of ER Ca^{2+}-ATPase, were used as agents inducing ER stress (Sigma, St. Louis, MO). 8-(*p*-sulfophenyl)-theophylline (8-SPT) was used as a nonselective adenosine receptor antagonist (Sigma). Anti-BiP/GRP78 and anti-CHOP/GADD153 antibodies were purchased from Santa Cruz Biotechnology (Santa Cruz, CA). Anti-caspase 12 and anti-α-actinin (sarcomeric) antibodies were purchased from Sigma. Anti-phosphorylated AMPK (Thr172), anti-AMPK, anti-phosphorylated eukaryotic elongation factor 2 (eEF2) (Thr56), anti-phosphorylated 4E binding protein 1 (4E-BP1) (Thr37/46), anti-phosphorylated eukaryotic initiation factor 2α (eIF2α) (Ser51), and anti-cleaved poly(ADP-ribose) polymerase (PARP) (Asp214) antibodies were purchased from Cell Signaling Technology (Beverly, MA). Anti-phosphorylated acetyl-coenzyme A carboxylase (ACC) (Ser79) was purchased from Upstate Biotechnology (Charlottesville, VA). Anti-α-tubulin monoclonal antibody was purchased from Calbiochem (Germany). All other chemicals were reagents of molecular biology grade obtained from standard commercial sources.

Cell culture and in vitro hypoxic model. Primary cultures of neonatal rat cardiomyocytes were prepared from ventricles of 1-day-old Wistar rats (Kiwa Jikken Dobutsu, Japan) as described previously (39). Care of all animals in the present study accorded with the Osaka University Animal Care guidelines. Briefly, hearts were treated with trypsin and collagenase for 30 min. Isolated cells were collected by centrifugation and resuspended in Medium 199 (M-199) containing 10% fetal calf serum (FCS). Cultures were enriched with myocytes by preplating for 90 min to deplete the population of nonmyocytes. Nonattached cells were plated onto plastic culture dishes at an appropriate cell density. The cells were cultured in M-199 containing 10% FCS at 37°C in 95% air-5% CO_2 for 30 h. The culture medium was then changed to fresh M-199 containing 1% FCS and cells were cultured for 16 h. Subsequently, the cells were treated with reagents or incubated in a hypoxic culture chamber. Medium was changed to fresh M-199 containing 1% FCS 1 h before exposure to reagents or hypoxia in order to obtain consistent ER stress response data (29).

Hypoxia was achieved by using an AnaeroPack System anaerobic jar (Mitsubishi Gas Chemical, Japan) equipped with an AnaeroPack (oxygen-absorbing and carbon dioxide-generating envelope) and a methylene blue indicator to monitor oxygen depletion. The AnaeroPack System is capable of depleting the concentration of oxygen down to <1% in 1 h and providing a 5% CO_2 atmosphere without changing medium pH. Cultured neonatal rat cardiomyocytes were subjected to hypoxic conditions in the anaerobic jar at 37°C for the time periods indicated, while controls were left in normoxic conditions at 37°C for the same time periods.

Generation of recombinant adenovirus and protocol for adenoviral infection. AMPK is an αβγ heterotrimer, the activation of which requires phosphorylation of threonine-172 on its catalytic α subunit. Therefore, cDNA encoding α1, which contains a mutation that changes threonine-172 to alanine, was used to construct the recombinant adenovirus expressing a dominant-negative form of the α1 subunit of AMPK (Ad-dnAMPK) according to a protocol described elsewhere (1). The cDNA was kindly donated by T. Kadowaki (Tokyo University, Tokyo, Japan) (66, 68).

We used adenovirus-mediated gene transfer to express this mutant in cultured primary rat cardiomyocytes. At 22 h after plating, cardiomyocytes were infected with adenovirus diluted in M-199 containing 10% FCS at a multiplicity of infection (MOI) of 20 and incubated for 8 h. After removal of viral suspension, cardiomyocytes were incubated with M-199 containing 1% FCS for 16 h and stimulated with reagents or exposed to hypoxia. Adenovirus vector expressing β-galactosidase (Ad-β-gal) was used as a control. Efficiency of infection, determined by *lacZ* gene expression in cultured cardiomyocytes, was consistently >90% with this method.

siRNA and transfection. Silencing of CHOP, caspase 12, and eEF2 kinase gene expression in primary neonatal rat cardiomyocytes was achieved by the small interfering RNA (siRNA) technique (12). The sequences of the siRNA duplexes were selected from the coding regions of the target mRNAs. Duplexes of 21-nucleotide siRNA with two 3′-overhanging TTs were designed and synthesized by Genedesign (Japan). The sense strand of siRNA used to silence the rat CHOP gene (CHOP siRNA) was CCUGUCCUCAGAUGAAAUUdTdT (where dT is deoxythymidine) (regions 172 to 192). The sense strand of siRNA used to silence the rat caspase 12 gene (caspase 12 siRNA) was GCACAUUC CUGGUCUUUAUdTdT (regions 743 to 763). The sense strand of siRNA used to silence the eEF2 kinase gene (eEF2 kinase siRNA) was GGCAGUCCAUG AUUUUAGUdTdT (regions 2116 to 2136). Nonspecific siRNA (ATCCGCGC GATAGTACGTAdTdT) was purchased from B-Bridge International (Japan) and used as a negative control (unrelated siRNA).

Transfection of cultured cardiomyocytes was carried out by electroporation using a Nucleofector device (Amaxa, Germany) according to proposed protocol (13). Briefly, after isolation of cardiomyocytes, 2×10^6 cardiomyocytes were resuspended in 100 μl of Nucleofector solution (rat cardiomyocyte Nucleofector

kit; Amaxa) together with 1.5 μg of a green fluorescent protein (GFP)-coding plasmid (pCMV-GFP) and 1.5 μg of siRNA duplexes for each target. The cells were then placed in an electroporation cuvette. Transfection of siRNA duplexes specific for each target transcript was carried out. Immediately after electroporation, 400 μl of prewarmed M-199 containing 10% FCS was added to the cuvette and the cells were transferred into culture plates containing prewarmed M-199 with 10% FCS. At the optimal time of gene silencing (48 h posttransfection), cells were exposed to reagents or hypoxia.

Western blot analysis. Neonatal rat cardiomyocytes were cultured at a cell density of 1×10^6 in 60-mm plastic culture dishes in duplicate. After culture with M-199 containing 10% FCS for 30 h, the medium was changed to M-199 containing 1% FCS and incubated for 16 h. Thereafter, cardiomyocytes were stimulated with reagents or incubated under hypoxic conditions. After stimulation, cells were immediately lysed in lysis buffer (62.5 mmol/liter Tris-HCl, pH 6.8; 2% [wt/vol] sodium dodecyl sulfate; 10% glycerol; 50 mmol/liter dithiothreitol; 0.1% bromophenol blue). The samples were separated on a 4% to 20% gradient polyacrylamide gel (Daiichi Kagaku, Japan), electrotransferred to a polyvinylidene difluoride membrane (Immobilon-P; Millipore, Bedford, MA), and processed for immunoblot analysis essentially as described previously (39). An enhanced chemiluminescence system was used for detection. Band intensity was analyzed using NIH image software (version 1.62).

Northern blot analysis. Portions (10 μg) of total RNA were prepared by the acid guanidinium thiocyanate–phenol-chloroform method. Total cellular RNA was loaded in each lane and size fractionated by 1% formaldehyde-agarose gel electrophoresis. Probes for BiP and CHOP were kindly donated by T. Katayama (Osaka University, Suita, Japan). Probes for ATF6 and XBP1 were kindly donated by K. Mori (Kyoto University, Kyoto, Japan). Probe for GAPDH (glyceraldehyde-3-phosphate dehydrogenase) was kindly donated by K. R. Chien (University of California, San Diego, CA). Probe for VEGF was generated as described previously (19). Band intensity was analyzed using NIH image software (version 1.62).

Immunostaining. For immunostaining, cardiomyocytes were grown on glass coverslips coated with gelatin. Cells were incubated under hypoxic conditions. Cells were fixed with 2% (wt/vol) formaldehyde for 15 min at room temperature and permeabilized with 0.1% Triton X-100–phosphate-buffered saline (PBS). Following three PBS washes, the glass coverslips were incubated in 1% bovine serum albumin-PBS for 1 h to block nonspecific binding sites. Subsequently, the cells were stained overnight at 4°C in 0.05% Tween 20 and 1% bovine serum albumin-PBS with primary antibodies for each target, followed by incubation for 1 h at room temperature with fluorescence-conjugated goat anti-mouse and goat anti-rabbit secondary antibodies. Then, the cells were stained with 0.5 mg/ml of Hoechst 33258 (Nacalai Tesque, Japan) to visualize nuclei. Cardiomyocytes were viewed by fluorescence microscopy, and pictures were taken using a Zeiss Axioskop2 (Carl Zeiss, Germany) with equal exposure times. To count positive cells for each primary antibody, a total of 200 to 300 Hoechst-stained nuclei (magnification of ×200) were counted for each experimental group. We measured the extent of fluorescence by using MetaMorpho microscope image analysis software (version 6.3; Molecular Devices, Japan). Cells with densities greater than the mean + standard deviation (SD) of the control group were considered positive.

Measurement of cell viability. Cells were plated at a density of 1×10^5 cells per well on 96-well plates for the 3-(4,5-dimethylthiazol-2-yl)-5-(3-carboxymethoxyphenyl)-2-(4-sulfophenyl)-2H-tetrazolium (MTS) assay. Cell viability was quantitated with an MTS cell respiratory assay (Promega, Madison, WI) according to the manufacturer's instructions. Viability was expressed as the absorbance at 490 nm measured with a spectrophotometer (Immuno-Mini NJ-2300; Inter Med, Japan).

Apoptosis assays. We used the cleaved PARP antibody for Western blot analyses and immunofluorescence analyses (52). PARP can be cleaved by many interleukin-converting enzyme-like caspases and is one of the main cleavage targets of caspase 3. Apoptosis was also confirmed by fluorescence microscope examination using Hoechst 33258 to visualize cell nuclei.

ATP measurement. Cells were plated at a density of 5×10^5 cells per well on 96-well plates. Intracellular ATP contents in cardiomyocytes were measured using an ATP assay kit (Calbiochem, Germany). After exposure to hypoxia or normoxia for the indicated time periods, culture medium was removed. Cells were treated with 100 μl of nuclear releasing reagent for 5 min at room temperature with gentle shaking. Then, the cell lysate was treated with 1 μl ATP monitoring enzyme. Luminescence was measured using FluorChem-IS8000 (Alpha Innotech Corporation, San Leandro, CA). Amounts of ATP were determined from a standard curve constructed with known concentrations of ATP. Decreases in ATP levels were determined by comparing these results with levels for the normoxic control.

Measurement of percent CPK. Cells were plated at a density of 1×10^6 cells per well onto 60-mm plastic culture dishes for the creatine phosphokinase (CPK) assay. Enzyme release determinations were made 30 h after exposure to hypoxia. Determination of CPK in cultured conditioned medium was performed with a commercially available kit (CPK2 kit; Wako, Japan) by monitoring absorbance changes at 560 nm. We then added 0.5 ml of 0.1% Triton X-100–PBS to the adherent cells on the 60-mm plastic culture dishes. After lysing pellets by incubating the cells for 5 min at 37°C and centrifuging for 2 min at 11,000 × *g*, we measured CPK activities from lysed cells as described above.

Leucine incorporation. For measurement of incorporation of [^{3}H]leucine, cells were plated at a density of 1×10^5 cells per well on 96-well plates. To examine the effects of AICAR on protein synthesis under hypoxic conditions, the cells were preincubated with or without AICAR, and then [^{3}H]leucine (1 μCi/ml) was added to the culture medium and the cells were exposed to hypoxia. The cells were washed three times with PBS and then treated with 5% trichloroacetic acid at 4°C for 10 min to precipitate proteins. The precipitates were dissolved in 0.1 N NaOH, and aliquots were tested with a scintillation counter.

Statistical analysis. Values are presented as means ± SDs. Statistical analysis was performed with the unpaired Student *t* test. Findings of P values of <0.05 were considered significant.

RESULTS

Induction of the unfolded protein responses in cultured neonatal rat cardiomyocytes after exposure to hypoxia. We first examined transcriptional and translational induction of an ER-specific chaperone, BiP, and a transcriptional factor, CHOP, both of which are markers of UPR (2, 71), in cultured neonatal rat cardiomyocytes under conditions of oxygen depletion. Cardiomyocytes were exposed to hypoxia in an anaerobic jar for various periods of time. Expression levels of BiP and CHOP mRNAs were induced by exposure to hypoxia (Fig. 1A). Expression levels of BiP and CHOP were also increased at the protein level during hypoxia (Fig. 1B). In contrast, neither BiP mRNA nor CHOP mRNA was induced under normoxic conditions (data not shown). Furthermore, we examined the expression levels of the upstream components of UPR (32, 69), ATF6 and XBP1, and a well-known hypoxia-inducible gene, the VEGF gene (33). ATF6 and XBP1 mRNA levels increased in a progressive manner during the time course (Fig. 1C). Both ATF6 and XBP1 mRNA expression levels followed a similar pattern to BiP, CHOP, and VEGF mRNA expression levels during the time periods. Because expression of ATF6, XBP1, BiP, and CHOP occurs specifically under conditions in which ER function is disturbed, these findings indicate that hypoxia disturbed ER function in cultured neonatal rat cardiomyocytes.

To confirm activation of UPR following exposure to hypoxia and to investigate the extent of UPR in each cell, we examined the expression levels of BiP and CHOP by use of immunohistochemical staining in cultured neonatal rat cardiomyocytes. Hypoxia increased the levels of expression of both BiP and CHOP proteins (Fig. 2). Higher magnification on microscopic examination revealed that BiP and CHOP proteins were immunostained in the paranuclear and nuclear regions of cardiomyocytes, respectively (Fig. 2A and B). BiP was constitutively expressed in the cytosol under control conditions but significantly increased in expression in the cytosol after exposure to hypoxia (Fig. 2A). On the other hand, CHOP was undetectable in most cells under normoxic conditions but was strongly induced in nuclei by hypoxia (Fig. 2B). Quantitative analysis revealed large numbers of BiP- or CHOP-positive cells among cardiomyocytes after exposure to hypoxia (Fig. 2C and D, respectively). We thus confirmed that UPR was induced by

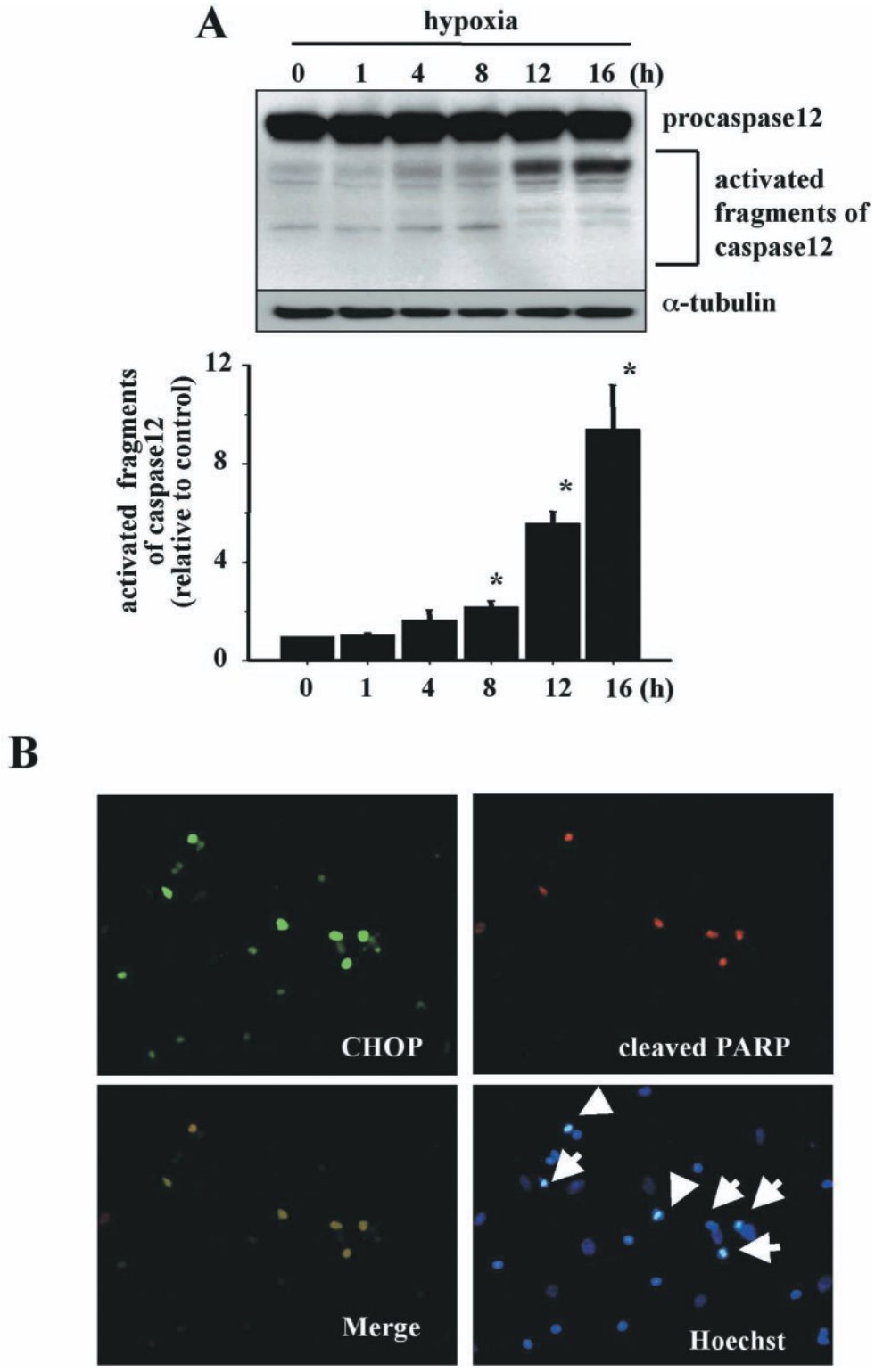

FIG. 3. ER stress-induced apoptotic signaling was detected after exposure to hypoxia in cardiomyocytes. (A) Cardiomyocytes were exposed to hypoxia for the indicated time periods. Whole-cell extracts were examined by Western blot analysis. The membranes were probed with antibodies specific for caspase 12. Densitometry was used to determine the ratios of band intensities for activated fragments of caspase 12 to band intensities for α-tubulin. Values are the means ± SDs from three independent experiments. *, P of <0.05 versus without hypoxia. (B) Fluorescence microscopy examination (original magnification of ×200) of cardiomyocytes exposed to hypoxia for 30 h and triply stained with anti-CHOP antibody, anti-cleaved PARP antibody, and Hoechst 33258. Images shown are representative findings from three independent experiments that had similar results. Note that the strong immunostaining of CHOP in nuclei colocalized with cleaved PARP immunostaining and condensed nuclei (arrows) revealed by Hoechst staining.

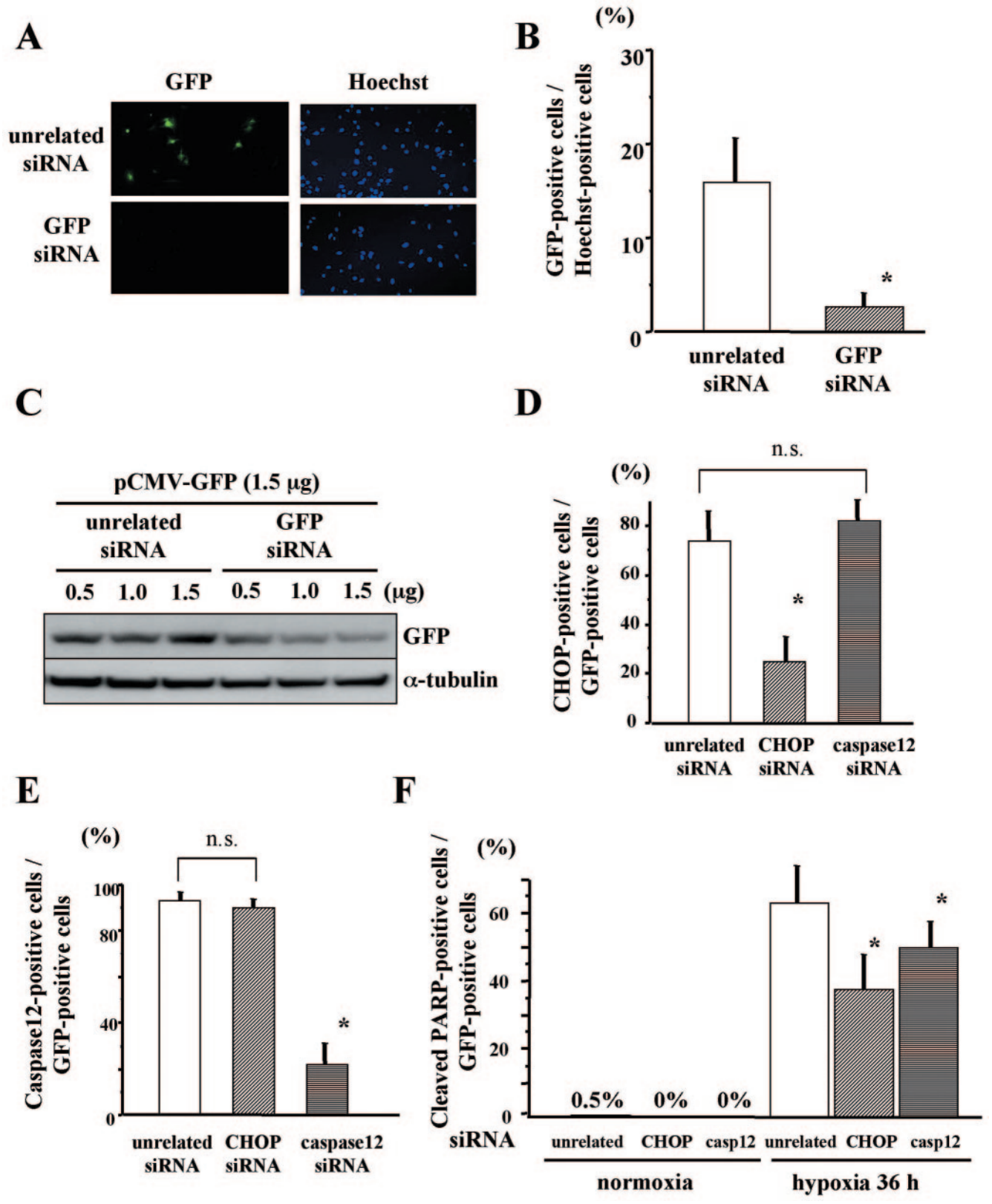

FIG. 4. Knockdown of CHOP and caspase 12 using siRNA duplexes yielded cardioprotection following exposure to hypoxia. (A and B) Neonatal rat cardiomyocytes were transfected with 1.5 μg of GFP siRNA together with 1.5 μg of pCMV-GFP as described in Materials and Methods. After 48 h of incubation on glass coverslips coated with gelatin, the cells were fixed and immunostained with anti-GFP antibody and Hoechst 33258 for nuclear staining. Knockdown of GFP was determined microscopically (original magnification of ×200). (C) Neonatal rat cardiomyocytes were transfected with the indicated doses of GFP siRNA duplexes together with 1.5 μg of pCMV-GFP as described in Materials and Methods. After 48 h of incubation, the cells

hypoxia in our model by demonstrating up-regulation of BiP and CHOP expression. Taken together, these findings suggest that ER stress is one of the pathological changes induced by hypoxia in cardiomyocytes.

Exposure to hypoxia induced ER stress-associated apoptotic signaling in cardiomyocytes. Because caspase 12, which is confined to the cytoplasmic side of the ER (46), is expressed at high levels in rat heart (45) and is believed to play an important role in ER stress-mediated cell death (46), we examined the activation of caspase 12 after exposure to hypoxia. As shown in Fig. 3A, caspase 12 was cleaved during hypoxia, indicating activation of caspase 12 in cardiomyocytes following exposure to hypoxia.

To clarify the involvement of ER stress in apoptotic cell death, double-fluorescence immunohistochemical staining of CHOP and cleaved PARP, a marker of apoptosis, was performed. Strong induction of CHOP during hypoxia colocalized with staining of cleaved PARP and condensed nuclei revealed by Hoechst staining (Fig. 3B), indicating that CHOP was associated with apoptosis.

Knockdown of CHOP and caspase 12 using siRNA duplexes yielded cardioprotective effects following exposure to hypoxia. To estimate transfection efficacy, 1.5 μg of a GFP-coding plasmid (pCMV-GFP) was cotransfected with 1.5 μg of unrelated siRNA duplexes or of siRNA duplexes cognate to GFP (GFP siRNA, purchased from Amaxa) by electroporation as described in Materials and Methods. After 48 h of incubation, cells were fixed and immunostained with anti-GFP antibody and with Hoechst 33258 for nuclear staining. We analyzed the findings for more than 300 Hoechst-stained cells and counted GFP-positive cells by fluorescence microscopy. A total of 16% of cardiomyocytes were transfected with pCMV-GFP. GFP siRNA duplexes efficiently suppressed transfected GFP gene expression, with an 83% reduction in the percentage of GFP-positive cells with GFP siRNA duplexes from that with unrelated siRNA duplexes (Fig. 4A and B). We also confirmed by Western blot analysis that GFP expression was barely detectable in GFP siRNA-transfected cardiomyocytes (Fig. 4C). It thus appeared that siRNA duplexes were almost completely transfected in cardiomyocytes transfected with pCMV-GFP and that GFP expression was a marker of transfection with siRNA duplexes.

To investigate whether siRNA duplexes for CHOP or caspase 12 knock down the target gene expression specifically, immunofluorescence experiments to determine target protein depletion were performed after exposure to 16 h of hypoxia. Figures 4D and E show that the CHOP siRNA and caspase 12 siRNA duplexes specifically reduced CHOP and caspase 12 expression levels, respectively, without modifying the expression levels of other proteins. No morphological changes were observed with phase-contrast micrographs of the CHOP siRNA- or caspase 12 siRNA-transfected cardiomyocytes under normoxic conditions (data not shown).

To confirm the effects of CHOP and caspase 12 knockout against hypoxic injury, after 48 h posttransfection with CHOP siRNA or caspase 12 siRNA duplexes, the cardiomyocytes were exposed to normoxia or hypoxia for 36 h. After fixing the cells, we counted GFP-positive cells undergoing apoptosis, which were labeled with the cleaved PARP antibody in nuclei by use of fluorescence microscopy. Figure 4F shows the percentages of cells undergoing apoptosis among GFP-positive cells. The expression of cleaved PARP was barely detectable in cardiomyocytes under normoxic conditions. Under conditions of hypoxia, the percentage was dramatically attenuated in CHOP siRNA- or caspase 12 siRNA-transfected cardiomyocytes compared to that in unrelated siRNA-transfected cardiomyocytes. These findings suggest that ER stress plays a role in inducing apoptosis during hypoxia.

AMPK protected cardiomyocytes against hypoxic injury through attenuation of ER stress. We investigated the roles played by AMPK during hypoxia in cultured neonatal rat cardiomyocytes. As shown in Fig. 5A, the exposure of cardiomyocytes to hypoxia resulted in rapid and sustained phosphorylation of AMPK and ACC, a downstream target of AMPK (24). We next assessed the activation of AMPK in cardiomyocytes in the presence or absence of AICAR, a chemical activator of AMPK. Western blot analysis revealed that exposure of cardiomyocytes to AICAR resulted in rapid phosphorylation of AMPK in a time-dependent (Fig. 5B) and dose-dependent (data not shown) fashion. Pretreatment with AICAR 1 h before exposure to hypoxia accelerated the phosphorylation status of AMPK during hypoxia compared with that in the untreated group (Fig. 5C).

To clarify whether AMPK promotes survival of cardiomyocytes in conditions yielding hypoxic injury, we performed an MTS cell respiration assay to assess cell viability and measured percent CPK release in culture medium to detect cell injury after exposure to hypoxia for 30 h. Relative MTS activity of the cells in the AICAR-pretreated group was significantly higher than that in the untreated group (Fig. 6A). Similarly, percent CPK release in the culture medium in the AICAR-pretreated group was significantly less than that in the untreated group (Fig. 6B). To confirm the effects of activation of AMPK by AICAR, we generated and performed infection of Ad-dnAMPK

were lysed, and GFP protein expression levels were examined by Western blot analysis. α-Tubulin was used as a control. (D and E) Neonatal rat cardiomyocytes were transfected with 1.5 μg of CHOP siRNA or caspase 12 siRNA duplexes together with 1.5 μg of pCMV-GFP as described in Materials and Methods. After 48 h of incubation on glass coverslips coated with gelatin, the cells were exposed to hypoxia for 16 h. Then, the cells were fixed and immunostained with anti-GFP and anti-CHOP (D) or anti-caspase 12 (E) antibodies. Quantitative analysis was performed using MetaMorpho microscope image analysis software. CHOP- and caspase 12-positive cells were defined as those with intensities greater than the mean + SD of the control group under normoxic conditions. (F) Neonatal rat cardiomyocytes were transfected with 1.5 μg of siRNA duplexes for each target together with 1.5 μg of pCMV-GFP as described in Materials and Methods. After 48 h of incubation on glass coverslips coated with gelatin, the cells were exposed to normoxia or hypoxia for 36 h and then fixed and immunostained with anti-GFP and anti-cleaved PARP antibodies, and stained with Hoechst 33258 for nuclei. The expression of cleaved PARP was barely detectable in cardiomyocytes under normoxic conditions. Images are representative findings from, and values are means ± SDs from, three independent experiments with similar results. Bars represent percentages of GFP-positive cells among Hoechst-positive cells (B) or percentages of CHOP-positive (D), caspase 12-positive (E), or cleaved PARP-positive cells (F) among GFP-positive cells. More than 100 Hoechst-stained (A and B) or GFP-positive cells (D to F) were examined in each experiment. *, P of <0.05 versus unrelated siRNA.

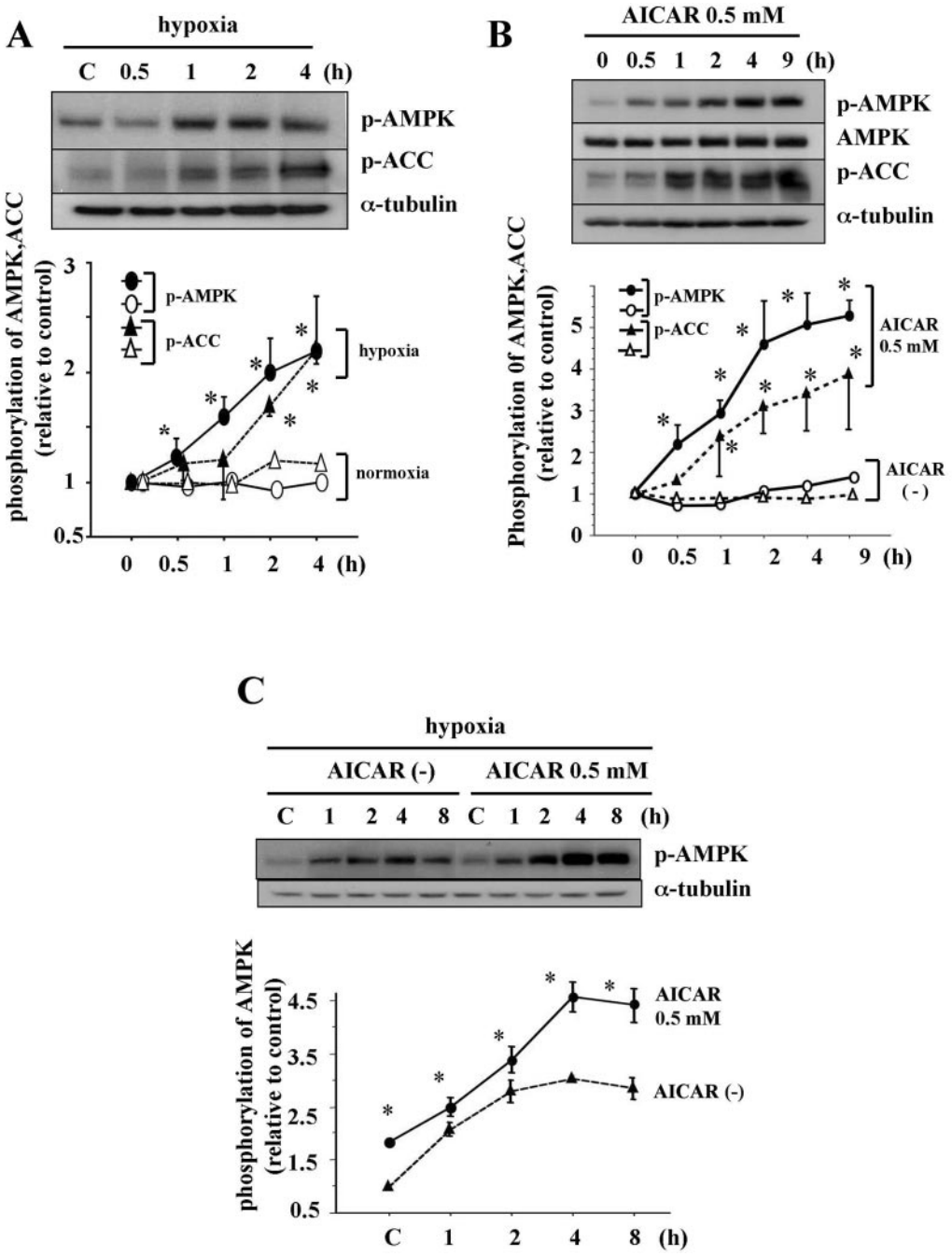

FIG. 5. AMPK was activated in cardiomyocytes during hypoxia and after treatment with AICAR. (A) As described in Materials and Methods, cardiomyocytes were incubated for the indicated time periods under normoxic or hypoxic conditions (A) or in the absence (−) or presence of 0.5 mM AICAR (B). For panel C, cardiomyocytes were treated or not with 0.5 mM of AICAR and 1 h later exposed to hypoxia for the indicated time periods. At each time point, the cells were lysed, and phosphorylation levels of AMPK (p-AMPK) and ACC (p-ACC) were determined by Western blot analysis. Membranes were reprobed with antibody to anti-α-tubulin to indicate equal protein loading. The graphs show the quantitative analyses. Densitometry was used to determine the ratios of band intensities for p-AMPK and p-ACC to band intensities for α-tubulin. All values are the means ± SDs from four independent experiments. *, P of <0.05 versus without hypoxia (A) or without AICAR (B and C).

in cardiomyocytes. Ad-dnAMPK (20 MOI) effectively blocked AICAR (0.5 mM)- and hypoxia-induced phosphorylation of ACC in cardiomyocytes (Fig. 6C). However, Ad-dnAMPK (20 MOI) did not completely block the activation of AMPK induced by more than 1 mM of AICAR (Fig. 6C). Figures 6D and E show that the protective effects of AICAR against hypoxia were abolished by overexpression of dnAMPK and that the inhibitory effects of Ad-dnAMPK were attenuated by a further dose of AICAR pretreatment, indicating that the cardioprotective effects of AICAR are mediated in an AMPK-dependent manner.

To examine whether AMPK protects cardiomyocytes against

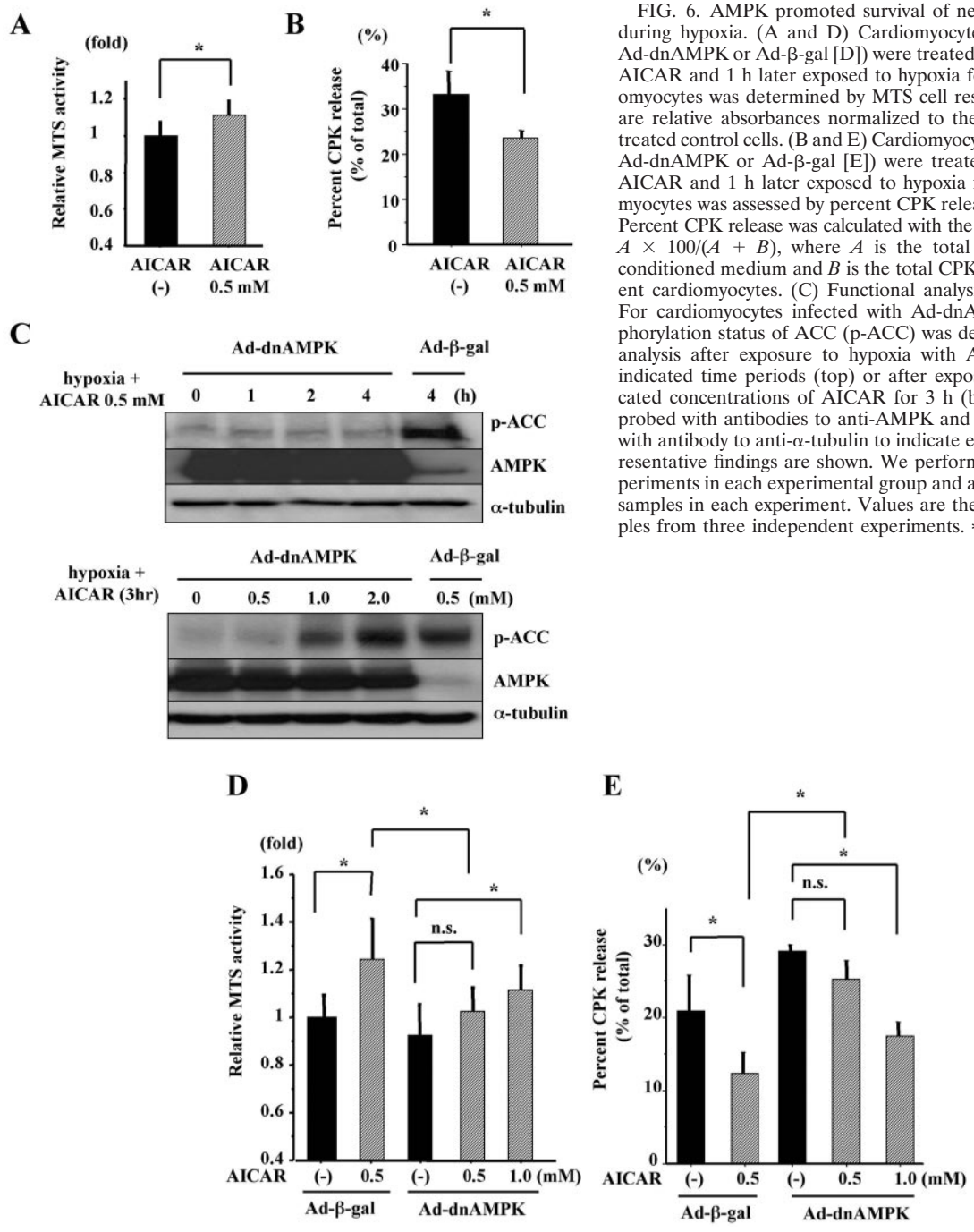

FIG. 6. AMPK promoted survival of neonatal rat cardiomyocytes during hypoxia. (A and D) Cardiomyocytes (some transfected with Ad-dnAMPK or Ad-β-gal [D]) were treated or not (−) with 0.5 mM of AICAR and 1 h later exposed to hypoxia for 30 h. Viability of cardiomyocytes was determined by MTS cell respiration assay, and values are relative absorbances normalized to the mean absorbance of untreated control cells. (B and E) Cardiomyocytes (some transfected with Ad-dnAMPK or Ad-β-gal [E]) were treated or not with 0.5 mM of AICAR and 1 h later exposed to hypoxia for 30 h. Injury of cardiomyocytes was assessed by percent CPK release in the culture medium. Percent CPK release was calculated with the formula % CPK release = $A \times 100/(A + B)$, where A is the total CPK activity in cultured conditioned medium and B is the total CPK activity from lysed adherent cardiomyocytes. (C) Functional analysis of Ad-dnAMPK. (Top) For cardiomyocytes infected with Ad-dnAMPK or Ad-β-gal, phosphorylation status of ACC (p-ACC) was determined by Western blot analysis after exposure to hypoxia with AICAR treatment for the indicated time periods (top) or after exposure to hypoxia with indicated concentrations of AICAR for 3 h (bottom). Membranes were probed with antibodies to anti-AMPK and anti-p-ACC and reprobed with antibody to anti-α-tubulin to indicate equal protein loading. Representative findings are shown. We performed three independent experiments in each experimental group and analyzed the findings for 16 samples in each experiment. Values are the means ± SDs of 48 samples from three independent experiments. ∗, $P < 0.05$.

hypoxia-induced apoptosis through attenuation of ER stress, we assessed the effects of AICAR on the extent and time course of induction of ER stress-associated proapoptotic signaling, such as that through CHOP and cleavage of caspase 12 during hypoxia. We also performed Western blot analysis of cell extracts by using anti-cleaved PARP antibody to assess cellular apoptosis. Pretreatment with AICAR attenuated the induction of CHOP mRNA (Fig. 7A) and protein (Fig. 7B to D) as well as cleavage of caspase 12 (Fig. 7B) during hypoxia. To confirm that these effects of AICAR were mediated in an AMPK-dependent manner, we examined the effects of AICAR on ER stress-mediated apoptotic signaling in cardiomyocytes infected with Ad-dnAMPK. Induction of CHOP and cleavage of caspase 12 were diminished by pretreatment with AICAR in Ad-β-gal-infected cardiomyocytes (Fig. 7E and G). In contrast, the effects of AICAR were abolished in Ad-dnAMPK-infected cardiomyocytes (Fig. 7F and H), indicating that the protective effects of AICAR against ER stress-associated apoptotic signaling are mediated in an AMPK-dependent manner. Moreover, as shown in Fig. 7I, pretreatment with AICAR significantly decreased the expression of cleaved PARP during hypoxia, and these cardioprotective effects of AICAR were abolished in

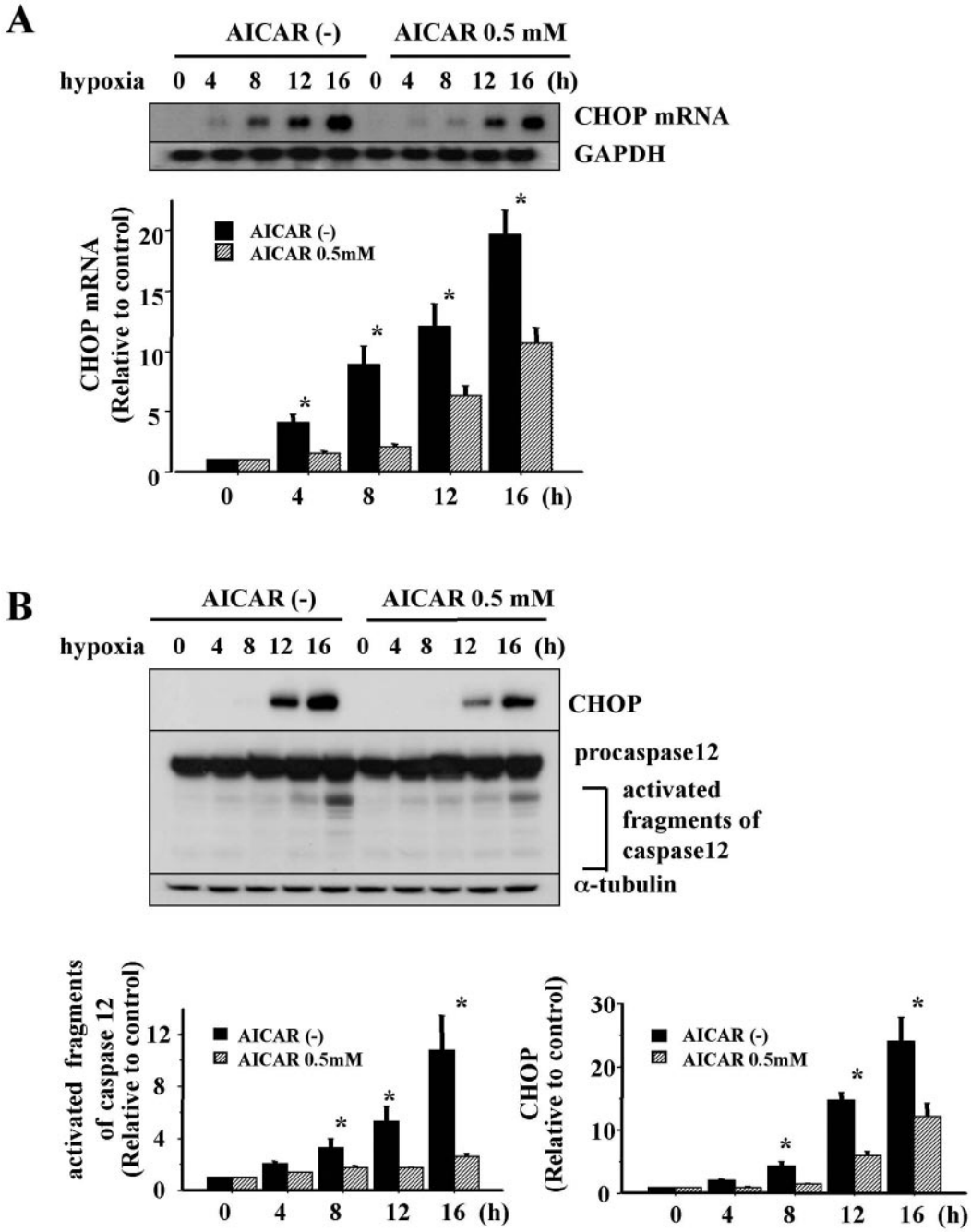

FIG. 7. AMPK delayed and attenuated ER-dependent death pathways during hypoxia. (A to D) Cardiomyocytes were treated or not (−) with 0.5 mM of AICAR and 1 h later exposed to hypoxia for the indicated time periods. Total RNA was isolated and subjected to Northern blot analysis with CHOP cDNA probes. Equal loading and transfer conditions were confirmed by GAPDH hybridization. (B) Whole-cell extracts of cells were examined by Western blot analysis. The membranes were probed with antibodies specific for CHOP and caspase 12. α-Tubulin was used as a control. (C) Cells were fixed and immunostained with anti-CHOP and anti-sarcomeric α-actinin antibodies and examined microscopically (original magnification of ×200). (D) Bars represent the percentages of CHOP-positive cells among α-actinin-positive cells. The intensity of CHOP staining in each cardiomyocyte was measured using MetaMorpho microscope image analysis software. CHOP-positive cells were defined as those with intensities greater than the mean + SD of the control group under normoxic conditions. More than 100 sarcomeric α-actinin-positive cells were examined for each experiment. (E to I) Cardiomyocytes were infected with Ad-β-gal (E and G) or Ad-dnAMPK (F and H) for 8 h. At 24 h after infection, the cells were treated or not with 0.5 mM of AICAR and 1 h later exposed to hypoxia for the indicated time periods. (E and F) Total RNA was isolated and subjected to Northern blot analysis using CHOP cDNA probe. Equal loading and transfer conditions were confirmed by GAPDH hybridization. (G and H) Whole-cell extracts of cells were examined by Western blot analysis. The membranes were probed with antibodies specific for CHOP and caspase 12. α-Tubulin was used as a control. (I) Whole-cell extracts were examined by Western blot analysis. The membranes were probed with antibody specific for cleaved PARP, a marker of apoptosis. Densitometry was used to determine the ratios of band intensities for CHOP to band intensities for GAPDH (A, E, and F) and the ratios of band intensities for CHOP, activated fragments of caspase 12 (B, G, and H), or PARP (I) to band intensities for α-tubulin. Images are representative findings from, and values are means ± SDs from, three independent experiments with similar results. *, P of <0.05 versus AICAR (0.5 mM) (A, B, and E to I) or versus without AICAR (C and D).

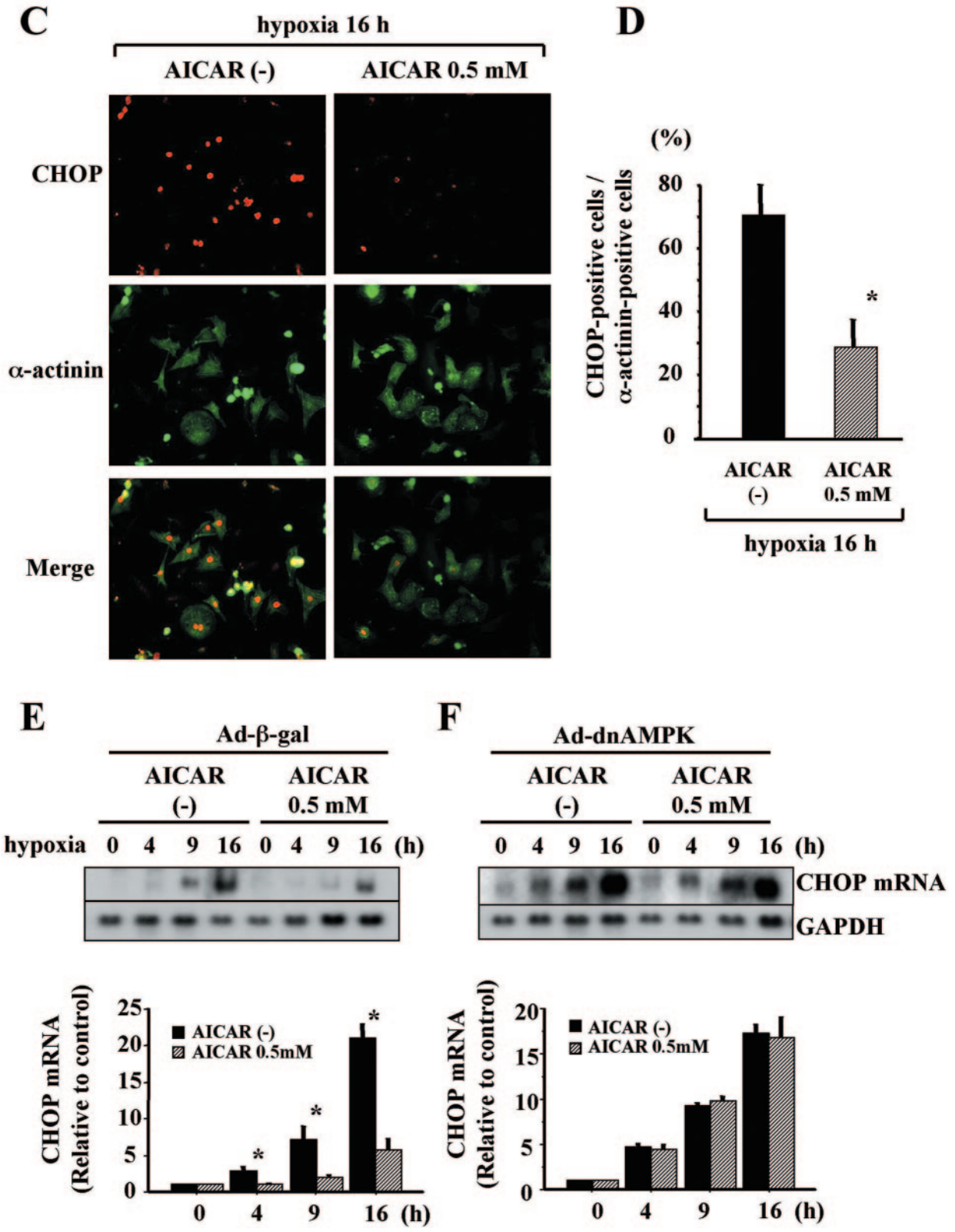

FIG. 7—*Continued.*

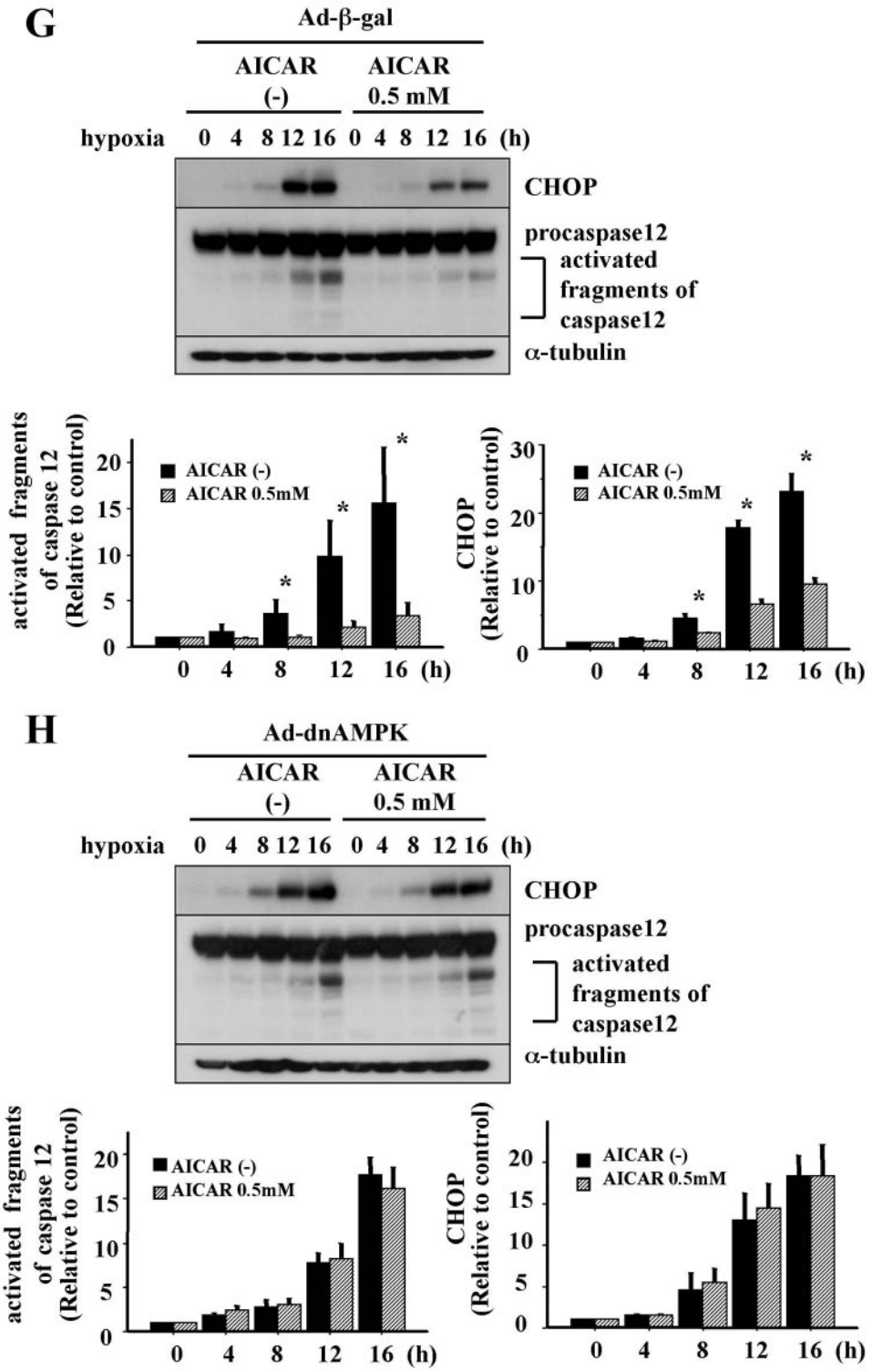

FIG. 7—*Continued.*

Ad-dnAMPK-infected cardiomyocytes. In addition, the inhibitory effects of dnAMPK were attenuated by a further dose of AICAR pretreatment. These findings indicate that pretreatment with AICAR diminishes apoptotic cell death and promotes survival.

Intracellular ATP content did not affect cardioprotection by AICAR during hypoxia. Depletion of intracellular ATP content is a crucial feature of ischemic processes, and degree of depression of ATP level is one of the determinants of apoptosis (9). Because AMPK is known to preserve energy during

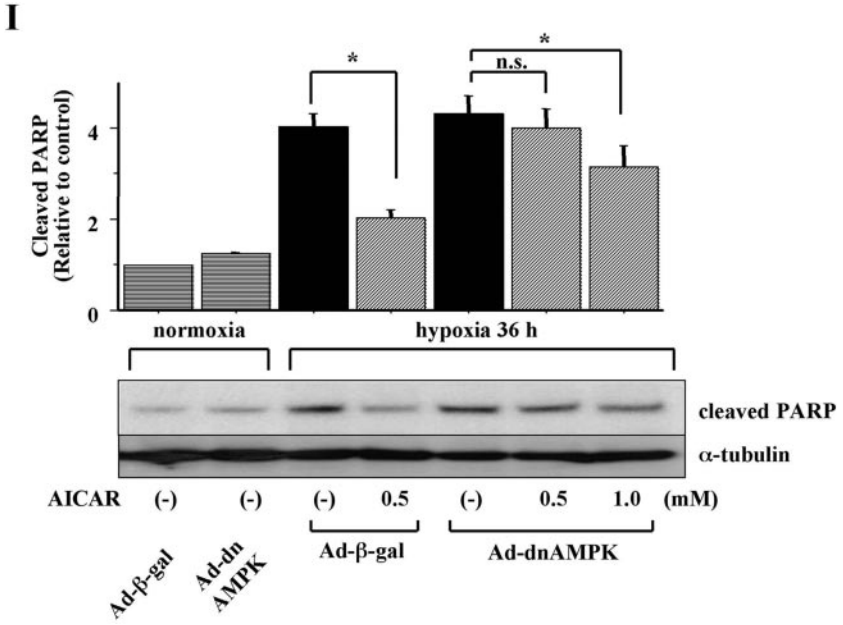

FIG. 7—*Continued.*

hypoxia (25), we examined whether the cardioprotective effects of AICAR against hypoxia-induced injury are due to AMPK-dependent ATP conservation during hypoxia. To investigate whether AICAR pretreatment preserves intracellular ATP content, ATP levels were measured after exposure of cardiomyocytes to hypoxia for various time periods in the presence or absence of AICAR. Figure 8 shows the time course of hypoxia-induced ATP depletion in cardiomyocytes. Intracellular ATP contents did not differ significantly between the AICAR-untreated group and the AICAR-pretreated group at either 10 h or 20 h after exposure to hypoxia. These findings indicate that the mechanism of cardioprotection by AICAR is not dependent on ATP conservation.

AMPK decreased the rate of protein synthesis during hypoxia via inactivation of eEF2. Recent reports have indicated that activation of AMPK leads to increased phosphorylation of eEF2, which inhibits elongation of translation in its phosphorylated state and thus leads to inhibition of protein synthesis in cardiomyocytes (28). We also confirmed that treatment of cardiomyocytes with 0.5 mM AICAR for 24 h caused inhibition of the protein synthesis rate by 21.5% under normoxic conditions, as assessed by examining incorporation of [^{3}H]leucine. Reduced rates of protein synthesis under conditions of ER stress serve to reduce the load of substrates presented to the folding machinery in the ER lumen, with mitigation of the consequences of insults to cellular homeostasis (53). We therefore hypothesized that regulation of eEF2 by AMPK might play a role in the attenuation of ER stress-associated apoptosis under conditions of hypoxia.

First, we measured the activities of key molecules related to translation, such as eEF2, 4E-BP1, and eIF2α, in cardiomyocytes during hypoxia. As shown in Fig. 9A, eIF2α, but not 4E-BP1, was phosphorylated during hypoxia. eEF2 was uniquely phosphorylated during hypoxia in biphasic fashion. Phosphorylation of eEF2 during hypoxia was significantly attenuated by Ad-dnAMPK (Fig. 9B), but phosphorylation of eIF2α during hypoxia was not attenuated by Ad-dnAMPK (data not shown). Moreover, as shown in Fig. 9C and D, AICAR phosphorylated eEF2, but not eIF2α, in a dose- and time-dependent fashion in cardiomyocytes. To further examine

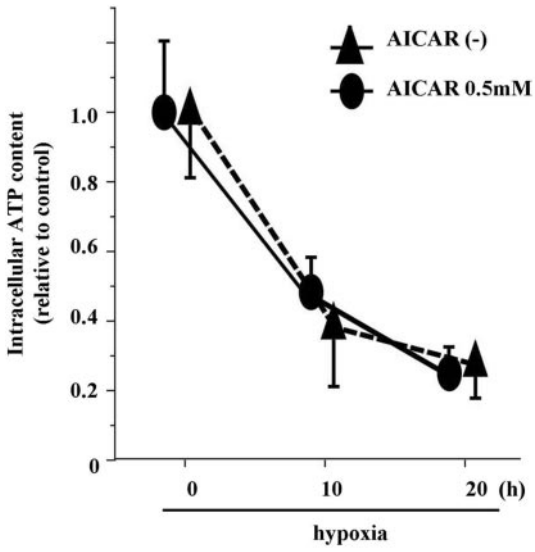

FIG. 8. AICAR did not increase intracellular ATP content during hypoxia. Values are intracellular ATP contents during hypoxia with or without (−) AICAR pretreatment. Intracellular ATP contents were measured for cardiomyocytes on 96-well plates as described in Materials and Methods. Cardiomyocytes were pretreated or not with 0.5 mM of AICAR and 1 h later exposed to hypoxia for the indicated time periods. Amounts of ATP were determined against a standard curve by using an ATP bioluminescence kit. Values are the means ± SDs from three independent experiments. No statistical significance was observed between the two groups at any time point.

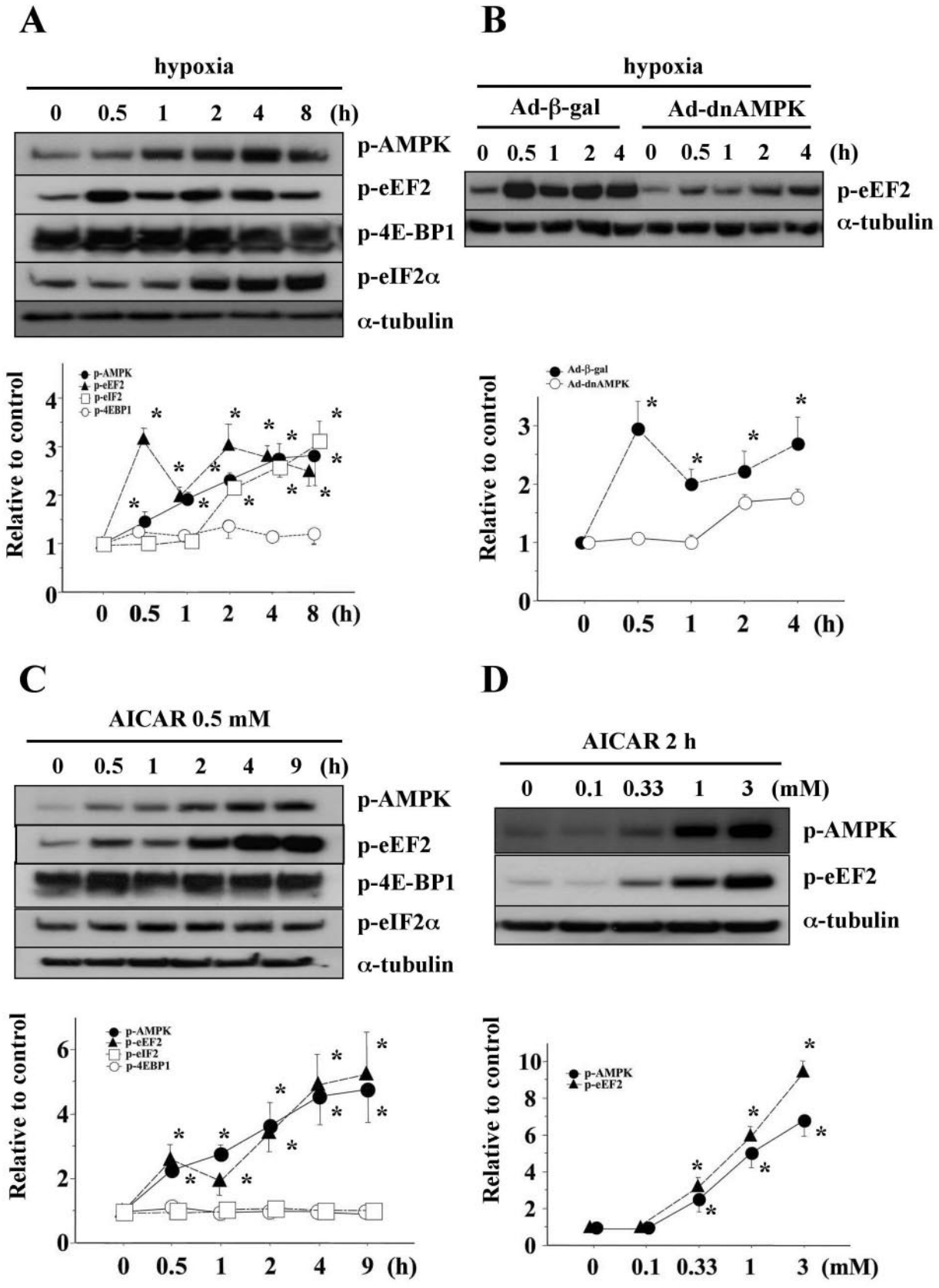
A
hypoxia
0 0.5 1 2 4 8 (h)
p-AMPK
p-eEF2
p-4E-BP1
p-eIF2α
α-tubulin
p-AMPK
p-eEF2
p-eIF2
p-4EBP1
Relative to control
0 0.5 1 2 4 8 (h)
B
hypoxia
Ad-β-gal
Ad-dnAMPK
0 0.5 1 2 4 0 0.5 1 2 4 (h)
p-eEF2
α-tubulin
Ad-β-gal
Ad-dnAMPK
Relative to control
0 0.5 1 2 4 (h)
C
AICAR 0.5 mM
0 0.5 1 2 4 9 (h)
p-AMPK
p-eEF2
p-4E-BP1
p-eIF2α
α-tubulin
p-AMPK
p-eEF2
p-eIF2
p-4EBP1
Relative to control
0 0.5 1 2 4 9 (h)
D
AICAR 2 h
0 0.1 0.33 1 3 (mM)
p-AMPK
p-eEF2
α-tubulin
p-AMPK
p-eEF2
Relative to control
0 0.1 0.33 1 3 (mM)

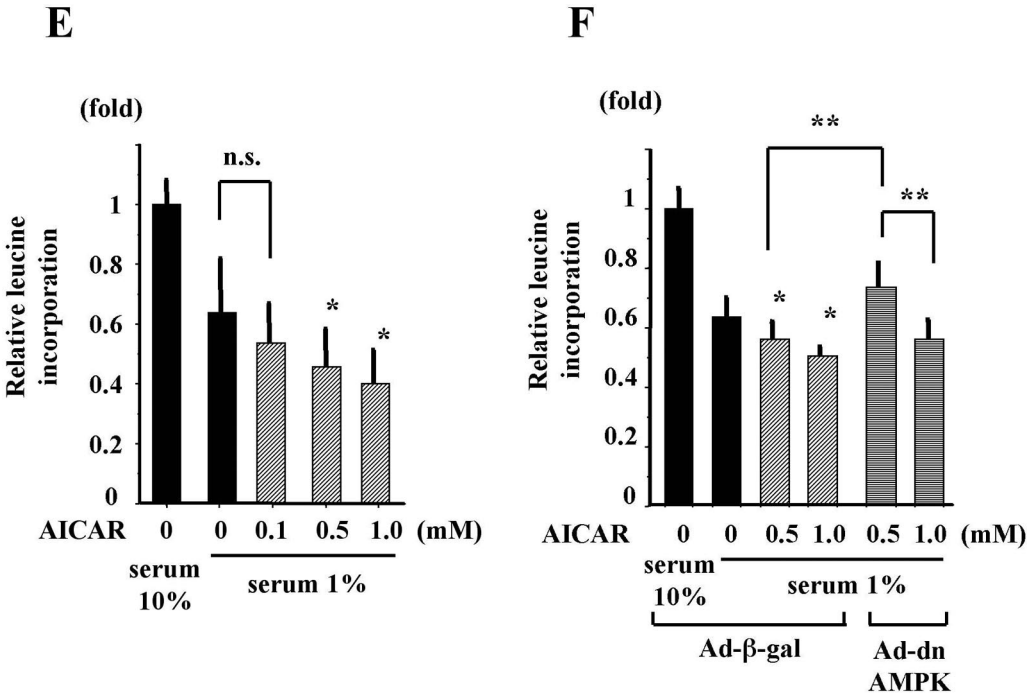

FIG. 9. AMPK attenuated protein synthesis via eEF2 during hypoxia. (A) Cardiomyocytes were exposed to hypoxia for the indicated time periods. At each time point, the cells were lysed, and the phosphorylation levels of eEF2, 4E-BP1, and eIF2α were examined by Western blot analysis. Membranes were probed with antibodies specific for p-eEF2, phosphorylated 4E-BP1 (p-4E-BP1), and phosphorylated eIF2α (p-eIF2α). *, P of <0.05 versus without hypoxia. (B) Cardiomyocytes were infected with Ad-β-gal or Ad-dnAMPK for 8 h. At 24 h after infection, the cells were exposed to hypoxia for the indicated time periods. Whole-cell extracts were examined by Western blot analysis. The membranes were probed with antibody specific for p-eEF2. α-Tubulin was used as a control. *, P of <0.05 versus Ad-β-gal at each time point. (C) Cardiomyocytes were treated with 0.5 mM of AICAR for the indicated time periods. At each time point, the cells were lysed, and phosphorylation levels of eEF2, 4E-BP1, and eIF2α were examined by Western blot analysis. Membranes were probed with antibodies specific for p-eEF2, p-4E-BP1, and p-eIF2α. *, P of <0.05 versus without hypoxia. (D) Cardiomyocytes were treated with indicated doses of AICAR for 2 h. The cells were lysed, and phosphorylation levels of AMPK and eEF2 were examined by Western blot analysis. *, P of <0.05 versus without AICAR. (E) Cardiomyocytes were treated or not with indicated doses of AICAR and 1 h later coincubated with [^{3}H]leucine (1 μCi/ml) and exposed to hypoxia for 8 h. Aliquots were tested with a scintillation counter. Bars represent the relative absorbance levels normalized to the mean absorbance level of untreated control cells (serum 10%). *, P of <0.05 versus without AICAR, serum 1%. n.s., not significant. (F) Cardiomyocytes were infected with Ad-β-gal or Ad-dnAMPK for 8 h. At 24 h after infection, the cells were treated or not with indicated doses of AICAR and 1 h later coincubated with [^{3}H]leucine (1 μCi/ml) and exposed to hypoxia for 8 h. Aliquots were tested with a scintillation counter. Bars represent the relative absorbance levels normalized to the mean absorbance level of untreated control cells (serum 10%). *, P of <0.05 versus Ad-β-gal, without AICAR, serum 1%. **, $P < 0.05$. We performed three independent experiments in each experimental group and analyzed the findings for 16 samples in each experiment. Values are the means ± SDs of 48 samples from three independent experiments. Densitometry was used to determine the ratios of band intensities for each target to band intensities for α-tubulin.

the effects of AMPK on protein synthesis during hypoxia, cardiomyocytes were exposed to hypoxia for 8 h with or without AICAR pretreatment and incorporation of [^{3}H]leucine was examined. The rate of protein synthesis during hypoxia was significantly and dose-dependently decreased by pretreatment with AICAR (Fig. 9E). This decrease in rate of protein synthesis was completely prevented by Ad-dnAMPK, and the inhibitory effects of dnAMPK were attenuated by a further dose of AICAR pretreatment (Fig. 9F).

Taken together, these findings suggest that AMPK might protect cardiomyocytes against ER stress-induced apoptosis during hypoxia via inhibition of protein synthesis through inactivation of eEF2.

Attenuation of eEF2 phosphorylation using eEF2 kinase siRNA duplexes abolished the cardioprotective effects of AICAR during hypoxia. To confirm that eEF2 plays a role in cardioprotection by AICAR during hypoxia, experiments with siRNA duplexes to attenuate the phosphorylation of eEF2 during hypoxia and AICAR treatment in cardiomyocytes were performed. Because eEF2 kinase is the only kinase that phosphorylates eEF2 (5), we suspected that knockdown of eEF2 kinase using siRNA duplexes would attenuate the phosphorylation of eEF2 during hypoxia and AICAR treatment. As shown in Fig. 10A, eEF2 kinase expression was specifically knocked down in eEF2 kinase siRNA-transfected cardiomyocytes. The fluorescence intensity of the eEF2 protein was affected in neither eEF2 kinase siRNA- nor unrelated siRNA-transfected cardiomyocytes (Fig. 10B). Fluorescent phosphorylated eEF2 (p-eEF2) production increased after 4 h of hypoxia with AICAR treatment in the unrelated siRNA-transfected cardiomyocytes (Fig. 10C). In contrast, fluorescent p-eEF2 production was abolished even after exposure to 4 h of hypoxia with AICAR treatment in eEF2 kinase siRNA-transfected cardiomyocytes (Fig. 10C), indicating that knockdown of eEF2 kinase attenuated the phosphorylation of eEF2 during

hypoxia with AICAR treatment. No morphological differences between eEF2 kinase siRNA- and unrelated siRNA-transfected cardiomyocytes were observed with phase-contrast micrographs under normoxic conditions (data not shown).

To investigate the roles played by eEF2 in mediating the cardioprotective effects of AICAR against hypoxia-induced ER stress and cell death, unrelated siRNA- or eEF2 kinase siRNA-transfected cardiomyocytes were incubated for 36 h under hypoxic conditions with or without pretreatment with AICAR. Cells under conditions of ER stress were assessed by immunofluorescence analyses with CHOP antibody using fluorescence microscopy. In addition, cells undergoing apoptosis were assessed by immunofluorescence analyses with cleaved PARP antibody using fluorescence microscopy. Pretreatment with AICAR dramatically decreased the percentage of CHOP-positive and cleaved PARP-positive cells in the unrelated siRNA-transfected cells (Fig. 10D and E). However, knockdown of eEF2 kinase abolished these cardioprotective effects of AICAR (Fig. 10D and E). These findings demonstrate that eEF2 inactivation plays a crucial role in mediating the cardioprotective effects of AICAR.

The cardioprotective effects of AICAR were not mediated by adenosine. AICAR has been proposed to increase tissue adenosine levels by entering the de novo nucleotide biosynthetic pathway (44), and several reports have indicated that the protective effects of AICAR are mediated by an adenosine-dependent mechanism (11). Therefore, to determine whether the protective effects of AICAR are independent of adenosine, we used 8-SPT as a nonselective adenosine receptor antagonist. The cytoprotective effects of AICAR were not diminished by 8-SPT (100 μM) (Fig. 11A and B), indicating that these effects are independent of adenosine.

AICAR attenuated Tm- and Tg-induced apoptotic signaling in cardiomyocytes. In cardiomyocytes, we found that BiP and CHOP were induced by ER stress inducers, including Tm and Tg, in a dose- and time-dependent fashion (data available on request) and that exposure to Tm and Tg induced the activation of caspase 12 (data available on request). Therefore, we examined whether AICAR attenuated Tm- and Tg-induced apoptotic signaling, as well as hypoxia-induced apoptotic signaling, in neonatal rat cardiomyocytes. As shown in Fig. 12A and B, induction of CHOP mRNA by Tm or Tg was significantly attenuated by pretreatment with AICAR 1 h before exposure to Tm or Tg, compared with results obtained with lack of pretreatment. These findings support the hypothesis that AMPK plays a cardioprotective role under conditions of ER stress.

DISCUSSION

In the present study, we first demonstrated that the ER-dependent apoptotic pathway is one of the mechanisms of hypoxic injury in cardiomyocytes. Furthermore, endogenous AMPK activation was found to protect cardiomyocytes against hypoxic injury through attenuation of ER stress. The mechanism by which AMPK protects cells during hypoxia attributes to suppression of protein synthesis due to phosphorylation of eEF2.

First, we found that hypoxic stress activated ER stress-dependent responses (Fig. 1 and 2) in cardiomyocytes. These observations indicate that hypoxia is capable of triggering activation of the ER-dependent signaling pathways in cardiomyocytes. Previous studies found that neuronal cells required both hypoxia and glucose deprivation for induction of UPR (45). However, in the present study, UPR were induced in cardiomyocytes in hypoxic conditions without glucose deprivation. These findings suggest that cardiomyocytes may be sensitive to ER stress. Interestingly, Okada et al. reported that pressure overload by transverse aortic constriction also induced UPR associated with cardiomyocyte apoptosis (48). Moreover, cytokines (6) and norepinephrine (37), both of which play roles in the pathophysiology of heart failure, also induce UPR, suggesting that ER stress plays a role in the pathophysiology of various heart diseases.

It has been established that ER stress both favors the survival of and induces apoptotic signaling in various types of cells. Therefore, the decision between survival and apoptosis may depend on the balance between survival signaling and apoptotic signaling. We examined whether ER stress-specific apoptotic signaling is involved in hypoxic injury of cardiomyocytes. Of the apoptotic pathways, three are known to be related to ER stress. The first is transcriptional induction of the gene for CHOP. Overexpression of CHOP promotes apoptosis, and deficiency of CHOP can protect cells from ER stress-induced apoptosis (49, 73), suggesting that CHOP is involved in the process of cell death caused by ER stress. The second is activation of caspase 12. Caspase 12 knockout mice exhibit resistance to ER stress (46), suggesting that caspase 12 also plays a role in the process of cell death caused by ER stress. The third is activation of the c-Jun NH2-terminal kinase (JNK) pathway (65), which is mediated by formation of the IRE1–tumor necrosis factor receptor-associated factor 2 (TRAF2)–apoptosis signal-regulating kinase 1 (ASK1) complex. Of these three components of the ER-related death pathways, induction of CHOP and activation of caspase 12 are ER-specific pathways. We therefore used these two pathways as markers of induction of the ER-specific death pathway. Furthermore, because all three ER death pathways eventually lead to the activation of caspase 3 (50), PARP, one of the main cleavage targets of caspase 3 (52), is considered a marker of cells undergoing apoptosis. In the present study, induction of CHOP and cleavage of caspase 12 increased in cardiomyocytes after exposure to hypoxia (Fig. 1A and B and 3A). Furthermore, as shown in Fig. 3B, in cardiomyocytes exposed to hypoxia, intense CHOP staining in nuclei colocalized with cleaved PARP staining and condensed nuclei as revealed by Hoechst staining. These findings indicate that hypoxic stress induced ER-dependent death pathway activity, leading to apoptosis. This theory is further supported by the observations that knockdown of ER death pathways such as that through CHOP and caspase 12 using siRNA duplexes led to cardioprotection after exposure to hypoxia (Fig. 4F).

The mechanisms of induction of the ER pathways after exposure to hypoxia have not been clearly determined. One proposed mechanism of ER stress induction during hypoxia is disruption of calcium homeostasis through inhibition of the sarcoplasmic/endoplasmic reticulum Ca^{2+}-ATPase pump due to intracellular ATP depletion (27). We therefore hypothesized that conservation of intracellular ATP content during hypoxia would protect cardiomyocytes from ER stress-induced cell death. Because AMPK acts as an intracellular energy sensor maintaining energy balance within cells during ischemia

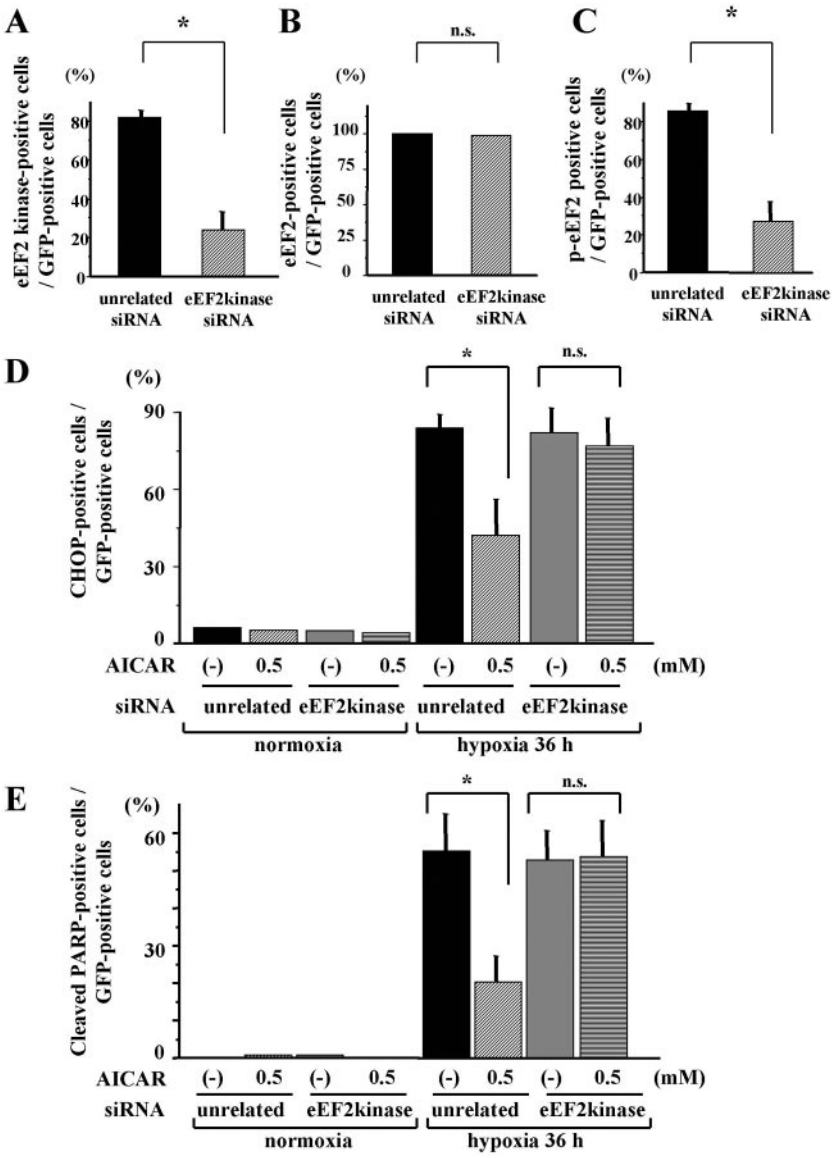

FIG. 10. Attenuation of eEF2 phosphorylation with eEF2 kinase siRNA abolished the cardioprotective effects of AICAR during hypoxia. (A to C) Cardiomyocytes were transfected with 1.5 μg of siRNA duplexes for eEF2 kinase together with 1.5 μg of pCMV-GFP as described in Materials and Methods. After 48 h of transfection on glass coverslips coated with gelatin, the cells were exposed to hypoxia with 0.5 mM AICAR for 4 h and then fixed and immunostained with anti-GFP and anti-eEF2 kinase (A), anti-eEF2 (B), or anti-p-eEF2 (C) antibodies. Quantitative analysis was performed using the MetaMorpho microscope image analysis software. Bars represent the percentages of eEF2 kinase- (A), eEF2- (B), or p-eEF2- (C) positive cells among GFP-positive cells. Positive cells for each target were defined as those with intensities greater than the mean + SD of the normoxic unrelated siRNA-transfected cells. Note that eEF2kinase siRNA efficiently attenuated the phosphorylation of eEF2 following exposure to hypoxia with 0.5 mM AICAR. n.s., not significant. (D and E) Neonatal rat cardiomyocytes transfected with pCMV-GFP and siRNA duplexes for eEF2 kinase or unrelated oligonucleotide were pretreated or not (−) with 0.5 mM AICAR and 1 h later exposed to hypoxia for 36 h. After fixing the cells, double-fluorescence immunohistochemical staining of CHOP (D) or cleaved PARP (E) and GFP and Hoechst staining were performed. Bars represent the percentages of CHOP-positive (D) or cleaved PARP-positive (E) cells among GFP-positive cells. Values are the means ± SDs from three independent experiments. More than 100 GFP-positive cells were examined in each experiment. *, $P < 0.05$.

(55), AMPK would be a potential candidate for the molecule that protects cells against ER stress-induced cell death during hypoxia. Moreover, recent studies have indicated that hypoxia itself regulates AMPK activity both independently of and dependently of intracellular AMP content (17), suggesting that AMPK also plays a role during mild ischemia that does not exist as a global change in high-energy phosphate homeostasis. Our findings showed that hypoxia activated AMPK and ACC in cultured cardiomyocytes (Fig. 5A) and that pretreatment with AICAR further activated AMPK and ACC (Fig. 5C), resulting in attenuation of hypoxic injury as assessed by MTS assay and percent CPK release in the culture medium due to AMPK activation (Fig. 6). Consistent with these findings, Russell et al. reported that the AMPK cascade protects cells against changes resulting from ischemia and reperfusion in perfused mouse hearts (54). Furthermore, AICAR has been shown to

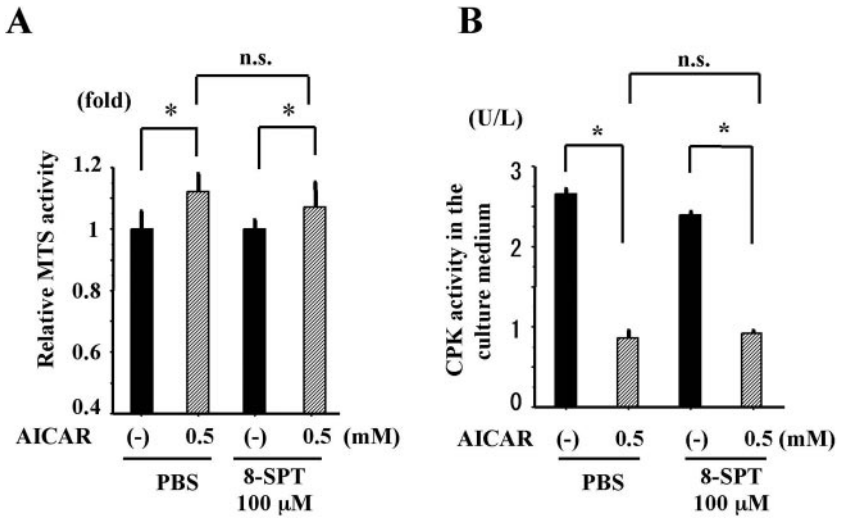

FIG. 11. AICAR protected cardiomyocytes against hypoxic stress independently of adenosine. Cardiomyocytes were treated or not (−) with 0.5 mM of AICAR and 100 μM of 8-SPT, a nonselective adenosine receptor antagonist, and 1 h later exposed to hypoxia for 30 h. (A) Viability of cardiomyocytes was determined by MTS cell respiration assay. Bars represent the relative absorbance levels normalized to the mean absorbance level of AICAR-free control cells. We performed three independent experiments in each experimental group and analyzed the findings for 16 samples in each experiment. (B) Injury of cardiomyocytes was assessed by CPK activity in the culture medium. Values are the means ± SDs from three independent experiments. *, $P < 0.05$. n.s., not significant.

exhibit cardioprotective effects in ischemic animal models as well as patients undergoing coronary-aortic bypass grafting (21, 36, 44). Therefore, our findings suggest that AICAR exhibits cardioprotective effects against hypoxic injury though AMPK-dependent mechanisms.

Moreover, pretreatment with AICAR significantly attenuated ER-specific death pathways during hypoxia, following suppression of cleavage of PARP (Fig. 7). These findings suggest that AICAR protects cardiomyocytes against hypoxia by attenuating ER stress-specific apoptosis via AMPK activation.

The question arises by which mechanisms AICAR-activated AMPK protects cells against hypoxia-induced ER-specific death pathways. It is known that AMPK favors fatty acid oxidation (31) and stimulates glycolysis by increasing glucose transport (47) and activating 6-phosphofructo-2 kinase (38), thereby promoting ATP production. We therefore first speculated that the cardioprotective effects of AICAR against activation of the hypoxia-induced ER-specific death pathway were due to conservation of intracellular ATP content. Surprisingly, however, the intracellular ATP content in AICAR-pretreated cells was essentially the same as that in AICAR-nontreated cells (Fig. 8). There are at least two possible explanations for this lack of difference in intracellular ATP levels between AICAR-pretreated and AICAR-nontreated cells. First, ATP is formed not only through mitochondrial oxidative phosphorylation but also through other metabolic pathways such as glycolysis and direct ADP phosphorylation by adenylate kinase (55). Inclusion of 5.5 mM glucose and 1% FCS in the culture medium may have provided cells with substrates for glycolytic ATP production and stimulated glycolytic ATP production in both groups of cells. Consistent with this hypothesis, Tatsumi et al. reported that when glucose was added to the medium, intracellular ATP content exhibited a corresponding increase during ischemia (62). Second, endogenous AMPK activation by hypoxia appears to be sufficient for preservation of intracellular ATP content, and a further increase in activation of AMPK by AICAR may thus exert no effects on preservation of intracellular ATP content during hypoxia. Although we could not exclude the possibility that small decreases in ATP level in crucial intracellular compartments not detected by measuring total cellular ATP content may have been responsible for the protective effects of AICAR, the beneficial effects of AICAR observed in this study appeared to be independent of total cellular ATP content. This conclusion is supported by the observations that preincubation with AICAR attenuated drug-induced ER stress, despite the presence of sufficient intracellular ATP content (Fig. 12).

What, then, are the mechanisms of protection by AMPK against hypoxic injury of cardiomyocytes? Recently, Chan and Dyck reported that AMPK suppresses protein synthesis via eEF2 inactivation in cardiomyocytes (8). Several studies reported that prior exposure of cells to an inhibitor of protein synthesis through translational initiation and elongation factors such as eIF2α (3, 35, 56), IF-4E (34), and EF1α (61) suppressed ER stress-induced cell death pathways. We therefore speculated that inactivation of a translational elongation factor such as eEF2 might suppress ER stress-induced cell death pathways. In fact, it has recently become clear that cells respond to stimuli that increase energy demand or reduce its supply in adapting to the environment by translational repression at the level of translational elongation (41), suggesting that elongation factors play a protective role under cellular stresses. The finding of a direct correlation between AMPK and eEF2 kinase (4) suggests that eEF2, a downstream target of eEF2 kinase, may play a role in mediating the cardioprotective effects of AICAR. As shown in Fig. 9B, increase in eEF2 phosphorylation after exposure to hypoxia was attenuated by Ad-dnAMPK. Furthermore, as shown in Fig. 9C and D, AICAR increased phosphorylation of eEF2, but not that of eIF2α and 4E-BP1, in a time- and dose-dependent fashion. As

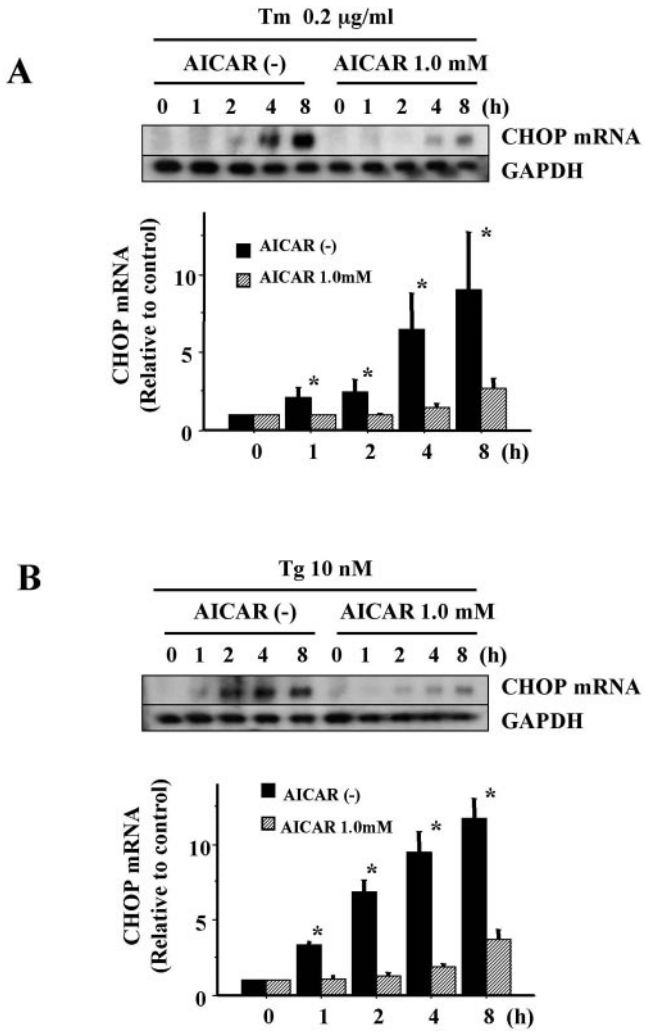

FIG. 12. AICAR pretreatment attenuated expression of CHOP mRNA induced by Tm or Tg. Cardiomyocytes were treated or not (−) with 1.0 mM of AICAR and 1 h later exposed to 0.2 μg/ml Tm (A) or 10 nM Tg (B) for the indicated time periods. Total RNA was isolated and subjected to Northern blot analysis with CHOP cDNA probes. Equal loading and transfer conditions were confirmed by GAPDH hybridization. Densitometry was used to determine the ratios of band intensities for CHOP to band intensities for GAPDH. Values are the means ± SDs from three independent experiments. *, P of <0.05 versus AICAR (1.0 mM) at each time point.

shown in Fig. 10A and C, increase in eEF2 phosphorylation after exposure to hypoxia with AICAR treatment was attenuated by eEF2 kinase siRNA. These findings suggest that eEF2 kinase, the only upstream kinase for eEF2 (5), is probably controlled by AMPK in cardiomyocytes during hypoxia.

We examined whether AICAR suppresses protein synthesis under our experimental conditions. As shown in Fig. 9E and F, AICAR significantly decreased the rate of protein synthesis during 8 h of hypoxia through AMPK activation. Because regulation of protein synthesis in mammalian cells is extremely complex, we could not rule out the possibility that other molecules play roles in hypoxia-induced suppression of protein synthesis. However, given the present findings, we speculate that eEF2 phosphorylation via AMPK-eEF2 kinase plays a role in mediating the cardioprotective effects of AICAR against hypoxia-induced ER stress. Although the effects of AICAR pretreatment on protein synthesis rate were small (Fig. 9E), a subtle inhibition of protein synthesis rate before ER dysfunction becomes apparent may be sufficient to suppress ER death pathways during hypoxia. Recent studies by Scheuner et al. (56) also suggest that a subtle increase in rate of protein synthesis through the reduction in eIF2α phosphorylation leads to β-cell failure and type 2 diabetes when an animal is exposed to ER stress.

In the present study, adenoviral overexpression of dnAMPK abolished the cardioprotective effect of AICAR (Fig. 6D and E and 7I), suggesting that this effect of AICAR is mediated by an AMPK-dependent mechanism. Because the cells we examined were isolated cardiomyocytes, we can exclude effects of adenosine on the vasculature on leukocytes. Furthermore, the cardioprotective effects of AICAR were not blocked by 8-SPT, a nonselective adenosine receptor antagonist, suggesting that the protective effects of AICAR were mediated by an adenosine-independent mechanism (Fig. 11A and B).

In conclusion, we found that ER-specific death pathways were induced by exposure to hypoxia in neonatal rat cardiomyocytes and that endogenous activation of AMPK by AICAR attenuated ER-specific death pathways and thus had antiapoptotic effects. The pathways that lead to cardioprotection against ER stress by AICAR are far from being understood in detail. Our findings indicate that AMPK-dependent phosphorylation of eEF2 may play a role in cardioprotective signaling mechanisms during hypoxia. Finally, we demonstrated that hypoxia is one of the metabolic stresses that can trigger ER death pathways in cardiomyocytes. Other cellular stresses, such as oxidative stress (26) and viral infection (60), have also been reported to be associated with ER stress. Cells of long-lived organs such as the heart are subjected to ER stress and must endure the consequences of accumulation of misfolded proteins in the ER over relatively long periods of time. Further studies of the ER death pathways in the heart should provide new insights into the pathogeneses of various heart diseases and lead to new therapeutic approaches to the prevention of such diseases.

ACKNOWLEDGMENTS

This study was supported by a Grant-in-Aid for Scientific Research from the Ministry of Education, Science, Sports, and Culture of Japan and by grants from the Takeda Science Foundation, the Mitsubishi Pharma Research Foundation, and the Pharmacological Research Foundation (Tokyo).

We thank Y. Takemura and K. Hamada for their expert technical assistance.

REFERENCES

1. **Becker, T. C., R. J. Noel, W. S. Coats, A. M. Gomez-Foix, T. Alam, R. D. Gerard, and C. B. Newgard.** 1994. Use of recombinant adenovirus for metabolic engineering of mammalian cells. Methods Cell Biol. **43:**161–189.
2. **Bertolotti, A., Y. Zhang, L. M. Hendershot, H. P. Harding, and D. Ron.** 2000. Dynamic interaction of BiP and ER stress transducers in the unfolded-protein response. Nat. Cell Biol. **2:**326–332.
3. **Boyce, M., K. F. Bryant, C. Jousse, K. Long, H. P. Harding, D. Scheuner, R. J. Kaufman, D. Ma, D. M. Coen, D. Ron, and J. Yuan.** 2005. A selective inhibitor of eIF2alpha dephosphorylation protects cells from ER stress. Science **307:**935–939.
4. **Browne, G. J., S. G. Finn, and C. G. Proud.** 2002. Stimulation of the AMP-activated protein kinase leads to activation of eukaryotic elongation factor 2 kinase and to its phosphorylation at a novel site, serine 398. J. Biol. Chem. **12:**12220–12231.

5. **Browne, G. J., and C. G. Proud.** 2002. Regulation of peptide-chain elongation in mammalian cells. Eur. J. Biochem. **269:**5360–5368.
6. **Cardozo, A. K., F. Ortis, J. Storling, Y.-M. Feng, J. Rasschaert, M. Tonnesen, F. Van Eylen, T. Mandrup-Poulsen, A. Herchuelz, and D. L. Eizirik.** 2005. Cytokines downregulate the sarcoendoplasmic reticulum pump Ca^{2+} ATPase 2b and deplete endoplasmic reticulum Ca^{2+}, leading to induction of endoplasmic reticulum stress in pancreatic β-cells. Diabetes **54:**452–461.
7. **Carling, D.** 2004. The AMP-activated protein kinase cascade—a unifying system for energy control. Trends Biochem. Sci. **29:**18–24.
8. **Chan, A. Y., and J. R. Dyck.** 2005. Activation of AMP-activated protein kinase (AMPK) inhibits protein synthesis: a potential strategy to prevent the development of cardiac hypertrophy. Can. J. Physiol. Pharmacol. **83:**24–28.
9. **Chen, S. J., M. E. Bradley, and T. C. Lee.** 1998. Chemical hypoxia triggers apoptosis of cultured neonatal rat cardiac myocytes: modulation by calcium-regulated proteases and protein kinases. Mol. Cell. Biochem. **178:**141–149.
10. **Crow, M. T., K. Mani, Y. J. Nam, and R. N. Kitsis.** 2004. The mitochondrial death pathway and cardiac myocyte apoptosis. Circ. Res. **95:**957–970.
11. **Donato, M., and R. J. Gelpi.** 2003. Adenosine and cardioprotection during reperfusion—an overview. Mol. Cell. Biochem. **251:**153–159.
12. **Elbashir, S. M., J. Harborth, W. Lendeckel, A. Yalcin, K. Weber, and T. Tuschl.** 2001. Duplexes of 21-nucleotide RNAs mediate RNA interference in cultured mammalian cells. Nature **411:**494–498.
13. **Elbashir, S. M., J. Harborth, K. Weber, and T. Tuschl.** 2002. Analysis of gene function in somatic mammalian cells using small interfering RNAs. Methods **26:**199–213.
14. **Ferri, K. F., and G. Kroemer.** 2001. Organelle-specific initiation of cell death pathways. Nat. Cell Biol. **3:**E255–E263.
15. **Forssmann, W. G., K. Nokihara, M. Gagelmann, D. Hock, S. Feller, P. Schulz-Knappe, and F. Herbst.** 1989. The heart is the center of a new endocrine, paracrine, and neuroendocrine system. Arch. Histol. Cytol. **52**(Suppl.)**:**293–315.
16. **Forssmann, W. G., R. Richter, and M. Meyer.** 1998. The endocrine heart and natriuretic peptides: histochemistry, cell biology, and functional aspects of the renal urodilatin system. Histochem. Cell Biol. **110:**335–357.
17. **Frederich, M., L. Zhang, and J. A. Balschi.** 2005. Hypoxia and AMP independently regulate AMP-activated protein kinase activity in heart. Am. J. Physiol. Heart Circ. Physiol. **288:**H2412–H2421.
18. **Fryer, L. G., A. Parbu-Patel, and D. Carling.** 2002. The anti-diabetic drugs rosiglitazone and metformin stimulate AMP-activated protein kinase through distinct signaling pathways. J. Biol. Chem. **277:**25226–25232.
19. **Funamoto, M., Y. Fujio, K. Kunisada, S. Negoro, E. Tone, T. Osugi, H. Hirota, M. Izumi, K. Yoshizaki, K. Walsh, T. Kishimoto, and K. Yamauchi-Takihara.** 2000. Signal transducer and activator of transcription 3 is required for glycoprotein 130-mediated induction of vascular endothelial growth factor in cardiac myocytes. J. Biol. Chem. **275:**10561–10566.
20. **Gollob, M. H., M. S. Green, A. S. Tang, T. Gollob, A. Karibe, A. S. Ali Hassan, F. Ahmad, R. Lozado, G. Shah, L. Fananapazir, L. L. Bachinski, and R. Roberts.** 2001. Identification of a gene responsible for familial Wolff-Parkinson-White syndrome. N. Engl. J. Med. **344:**1823–1831.
21. **Gruber, H. E.** 1994. Acadesine: preclinical overview. Adv. Exp. Med. Biol. **370:**423–426.
22. **Hardie, D. G.** 2003. Minireview: the AMP-activated protein kinase cascade: the key sensor of cellular energy status. Endocrinology **144:**5179–5183.
23. **Hardie, D. G.** 2004. AMP-activated protein kinase: the guardian of cardiac energy status. J. Clin. Investig. **114:**465–468.
24. **Hardie, D. G., and D. Carling.** 1997. The AMP-activated protein kinase-fuel gauge of the mammalian cell? Eur. J. Biochem. **246:**259–273.
25. **Hardie, D. G., D. Carling, and M. Carlson.** 1998. The AMP-activated/SNF1 protein kinase subfamily: metabolic sensors of the eukaryotic cell? Annu. Rev. Biochem. **67:**821–855.
26. **Hayashi, T., A. Saito, S. Okuno, M. Ferrand-Drake, R. L. Dodd, and P. H. Chan.** 2003. Oxidative injury to the endoplasmic reticulum in mouse brains after transient focal ischemia. Neurobiol. Dis. **23:**229–239.
27. **Heaps, C. L., M. Sturek, E. M. Price, M. H. Laughlin, and J. L. Parker.** 2001. Sarcoplasmic reticulum Ca^{2+} uptake is impaired in coronary smooth muscle distal to coronary occlusion. Am. J. Physiol. Heart Circ. Physiol. **281:**H223–H231.
28. **Horman, S., C. Beauloye, D. Vertommen, J. L. Vanoverschelde, L. Hue, and M. H. Rider.** 2003. Myocardial ischemia and increased heart work modulate the phosphorylation state of eukaryotic elongation factor-2. J. Biol. Chem. **278:**41970–41976.
29. **Imaizumi, K., T. Katayama, and M. Tohyama.** 2000. Presenilin and the UPR. Nat. Cell Biol. **85:**E104.
30. **Kaufman, R. J.** 2002. Orchestrating the unfolded protein response in health and disease. J. Clin. Investig. **110:**1389–1398.
31. **Kudo, N., A. J. Barr, R. L. Barr, S. Desai, and G. D. Lopaschuk.** 1995. High rates of fatty acid oxidation during reperfusion of ischemic hearts are associated with a decrease in malonyl-CoA levels due to an increase in 5′-AMP-activated protein kinase inhibition of acetyl-CoA carboxylase. J. Biol. Chem. **270:**17513–17520.
32. **Lee, K., W. Tirasophon, X. Shen, M. Michalak, R. Prywes, T. Okada, H. Yoshida, K. Mori, and R. J. Kaufman.** 2002. IRE1-mediated unconventional mRNA splicing and S2P-mediated ATF6 cleavage merge to regulate XBP1 in signaling the unfolded protein response. Genes Dev. **16:**452–466.
33. **Levy, A. P., N. S. Levy, J. Loscalzo, A. Calderone, N. Takahashi, K.-T. Yeo, G. Koren, W. S. Colucci, and M. A. Goldberg.** 1995. Regulation of vascular endotherial growth factor in cardiac myocytes. Circ. Res. **76:**758–766.
34. **Li, S., D. M. Perlman, M. S. Peterson, D. Burrichter, S. Avdulov, V. A. Polunovsky, and P. B. Bitterman.** 2004. Translation initiation factor 4E blocks endoplasmic reticulum-mediated apoptosis. J. Biol. Chem. **279:**21312–21317.
35. **Lu, P. D., C. Jousse, S. J. Marciniak, Y. Zhang, I. Novoa, D. Scheuner, R. J. Kaufman, D. Ron, and H. P. Harding.** 2004. Cytoprotection by pre-emptive conditional phosphorylation of translation initiation factor 2. EMBO J. **23:**169–179.
36. **Mangano, D. T., et al.** 1997. Effects of acadesine on myocardial infarction, stroke, and death following surgery. A meta-analysis of the 5 international randomized trials. JAMA **277:**325–332.
37. **Mao, W., C. Iwai, F. Qin, and C. S. Liang.** 2005. Norepinephrine induces endoplasmic reticulum stress and downregulation of norepinephrine transporter density in PC12 cells via oxidative stress. Am. J. Physiol. Heart Circ. Physiol. **288:**H2381–H2389.
38. **Marsin, A. S., L. Bertrand, M. H. Rider, J. Deprez, C. Beauloye, M. F. Vincent, G. Van den Berghe, D. Carling, and L. Hue.** 2000. Phosphorylation and activation of heart PFK-2 by AMPK has a role in the stimulation of glycolysis during ischaemia. Curr. Biol. **10:**1247–1255.
39. **Masaki, M., M. Izumi, Y. Oshima, Y. Nakaoka, T. Kuroda, R. Kimura, S. Sugiyama, K. Terai, M. Kitakaze, K. Yamauchi-Takihara, I. Kawase, and H. Hirota.** 2005. Smad1 protects cardiomyocytes from ischemia-reperfusion injury. Circulation **111:**2752–2759.
40. **Masoudi, F. A., S. E. Inzucchi, Y. Wang, E. P. Havranek, J. M. Foody, and H. M. Krumholz.** 2005. Thiazolidinediones, metformin, and outcomes in older patients with diabetes and heart failure: an observational study. Circulation **111:**583–590.
41. **McLeod, L. E., and C. G. Proud.** 2002. ATP depletion increases phosphorylation of elongation factor eEF2 in adult cardiomyocytes independently of inhibition of mTOR signalling. FEBS Lett. **531:**448–452.
42. **Minokoshi, Y., Y. B. Kim, O. D. Peroni, L. G. Fryer, C. Muller, D. Carling, and B. B. Kahn.** 2002. Leptin stimulates fatty-acid oxidation by activating AMP-activated protein kinase. Nature **415:**339–343.
43. **Mori, K.** 2000. Tripartite management of unfolded proteins in the endoplasmic reticulum. Cell **101:**451–454.
44. **Mullane, K.** 1993. Acadesine: the prototype adenosine regulating agent for reducing myocardial ischaemic injury. Cardiovasc. Res. **27:**43–47.
45. **Nakagawa, T., and J. Yuan.** 2000. Cross-talk between two cysteine protease families. Activation of caspase-12 by calpain in apoptosis. J. Cell Biol. **150:**887–894.
46. **Nakagawa, T., H. Zhu, N. Morishima, E. Li, J. Xu, B. A. Yankner, and J. Yuan.** 2000. Caspase-12 mediates endoplasmic-reticulum-specific apoptosis and cytotoxicity by amyloid-beta. Nature **403:**98–103.
47. **Nishino, Y., T. Miura, T. Miki, J. Sakamoto, Y. Nakamura, Y. Ikeda, H. Kobayashi, and K. Shimamoto.** 2004. Ischemic preconditioning activates AMPK in a PKC-dependent manner and induces GLUT4 up-regulation in the late phase of cardioprotection. Cardiovasc. Res. **61:**610–619.
48. **Okada, K., T. Minamino, Y. Tsukamoto, Y. Liao, O. Tsukamoto, S. Takashima, A. Hirata, M. Fujita, Y. Nagamachi, T. Nakatani, C. Yutani, K. Ozawa, S. Ogawa, H. Tomoike, M. Hori, and M. Kitakaze.** 2004. Prolonged endoplasmic reticulum stress in hypertrophic and failing heart after aortic constriction: possible contribution of endoplasmic reticulum stress to cardiac myocyte apoptosis. Circulation **110:**705–712.
49. **Oyadomari, S., A. Koizumi, K. Takeda, T. Gotoh, S. Akira, E. Araki, and M. Mori.** 2002. Targeted disruption of the *Chop* gene delays endoplasmic reticulum stress-mediated diabetes. J. Clin. Investig. **109:**525–532.
50. **Oyadomari, S., and M. Mori.** 2004. Roles of CHOP/GADD153 in endoplasmic reticulum stress. Cell Death Diff. **11:**381–389.
51. **Ozawa, K., T. Kondo, O. Hori, Y. Kitao, D. M. Stern, W. Eisenmenger, S. Ogawa, and T. Ohshima.** 2001. Expression of the oxygen-regulated protein ORP150 accelerates wound healing by modulating intracellular VEGF transport. J. Clin. Investig. **108:**41–50.
52. **Pieper, A. A., A. Verma, J. Zhang, and S. H. Snyder.** 1999. Poly (ADP-ribose) polymerase, nitric oxide and cell death. Trends Pharmacol. Sci. **20:**171–181.
53. **Ron, D.** 2002. Translational control in the endoplasmic reticulum stress response. J. Clin. Investig. **110:**1383–1388.
54. **Russell, R. R., III, J. Li, D. L. Coven, M. Pypaert, C. Zechner, M. Palmeri, F. J. Giordano, J. Mu, M. J. Birnbaum, and L. H. Young.** 2004. AMP-activated protein kinase mediates ischemic glucose uptake and prevents postischemic cardiac dysfunction, apoptosis, and injury. J. Clin. Investig. **114:**495–503.
55. **Sambandam, N., and G. D. Lopaschuk.** 2003. AMP-activated protein kinase (AMPK) control of fatty acid and glucose metabolism in the ischemic heart. Prog. Lipid Res. **42:**238–256.
56. **Scheuner, D., D. V. Mierde, B. Song, D. Flamez, J. W. M. Creemers, K. Tsukamoto, M. Ribick, F. C. Schuit, and R. J. Kaufman.** 2005. Control of

mRNA translation preserves endoplasmic reticulum function in beta cells and maintains glucose homeostasis. Nat. Med. **11:**757–764.

57. **Shannon, T. R., and D. M. Bers.** 2004. Integrated Ca^{2+} management in cardiac myocytes. Ann. N. Y. Acad. Sci. **1015:**28–38.
58. **Shibata, R., N. Ouchi, M. Ito, S. Kihara, I. Shiojima, D. R. Pimentel, M. Kumada, K. Sato, S. Schiekofer, K. Ohashi, T. Funahashi, W. S. Colucci, and K. Walsh.** 2004. Adiponectin-mediated modulation of hypertrophic signals in the heart. Nat. Med. **10:**1384–1389.
59. **Stapleton, D., K. I. Mitchelhill, G. Gao, J. Widmer, B. J. Michell, T. Teh, C. M. House, C. S. Fernandez, T. Cox, L. A. Witters, and B. E. Kemp.** 1996. Mammalian AMP-activated protein kinase subfamily. J. Biol. Chem. **271:** 611–614.
60. **Su, H.-L., C.-L. Liao, and Y.-L. Lin.** 2002. Japanese encephalitis virus infection initiates endoplasmic reticulum stress and an unfolded protein response. J. Virol. **76:**4162–4171.
61. **Talapatra, S., J. D. Wagner, and C. B. Thompson.** 2002. Elongation factor-1 alpha is a selective regulator of growth factor withdrawal and ER stress-induced apoptosis. Cell Death Diff. **9:**856–861.
62. **Tatsumi, T., J. Shiraishi, N. Keira, K. Akashi, A. Mano, S. Yamanaka, S. Matoba, S. Fushiki, H. Fliss, and M. Nakagawa.** 2003. Intracellular ATP is required for mitochondrial apoptotic pathways in isolated hypoxic rat cardiac myocytes. Cardiovasc. Res. **59:**428–440.
63. **Tian, R., N. Musi, J. D'Agostino, M. F. Hirshman, and L. J. Goodyear.** 2001. Increased adenosine monophosphate-activated protein kinase activity in rat hearts with pressure-overload hypertrophy. Circulation **104:**1664–1669.
64. **Travers, K. J., C. K. Patil, L. Wodicka, D. J. Lockhart, J. S. Weissman, and P. Walter.** 2000. Functional and genomic analyses reveal an essential coordination between the unfolded protein response and ER-associated degradation. Cell **101:**249–258.
65. **Urano, F., X. Wang, A. Bertolotti, Y. Zhang, P. Chung, H. P. Harding, and D. Ron.** 2000. Coupling of stress in the ER to activation of JNK protein kinases by transmembrane protein kinase IRE1. Science **287:**664–666.
66. **Woods, A., D. Azzout-Marniche, M. Foretz, S. C. Stein, P. Lemarchand, P. Ferré, F. Foufelle, and D. Carling.** 2000. Characterization of the role of AMP-activated protein kinase in the regulation of glucose-activated gene expression using constitutively active and dominant negative forms of the kinase. Mol. Cell. Biol. **20:**6704–6711.
67. **Xing, Y., N. Musi, N. Fujii, L. Zou, I. Luptak, M. F. Hirshman, L. J. Goodyear, and R. Tian.** 2003. Glucose metabolism and energy homeostasis in mouse hearts overexpressing dominant negative alpha2 subunit of AMP-activated protein kinase. J. Biol. Chem. **278:**28372–28377.
68. **Yamauchi, T., J. Kamon, Y. Minokoshi, Y. Ito, H. Waki, S. Uchida, S. Yamashita, M. Noda, S. Kita, K. Ueki, K. Eto, Y. Akanuma, P. Froguel, F. Foufelle, P. Ferre, D. Carling, S. Kimura, R. Nagai, B. B. Kahn, and T. Kadowaki.** 2002. Adiponectin stimulates glucose utilization and fatty-acid oxidation by activating AMP-activated protein kinase. Nat. Med. **8:**1288–1295.
69. **Yoshida, H., T. Matsui, A. Yamamoto, T. Okada, and K. Mori.** 2001. XBP1 mRNA is induced by ATF6 and spliced by IRE1 in response to ER stress to produce a highly active transcription factor. Cell **107:**881–891.
70. **Yoshida, H., T. Matsui, N. Hosokawa, R. J. Kaufman, K. Nagata, and K. Mori.** 2003. A time-dependent phase shift in the mammalian unfolded protein response. Dev. Cell **4:**265–271.
71. **Zhang, K., and R. J. Kaufman.** 2003. Signaling the unfolded protein response from the endoplasmic reticulum. J. Biol. Chem. **23:**25935–25938.
72. **Zhou, G., R. Myers, Y. Li, Y. Chen, X. Shen, J. Fenyk-Melody, M. Wu, J. Ventre, T. Doebber, N. Fujii, N. Musi, M. F. Hirshman, L. J. Goodyear, and D. E. Moller.** 2001. Role of AMP-activated protein kinase in mechanism of metformin action. J. Clin. Investig. **108:**1167–1174.
73. **Zinszner, H., M. Kuroda, X. Wang, N. Batchvarova, R. T. Lightfoot, H. Remotti, J. L. Stevens, and D. Ron.** 1998. CHOP is implicated in programmed cell death in response to impaired function of the endoplasmic reticulum. Genes Dev. **12:**982–995.